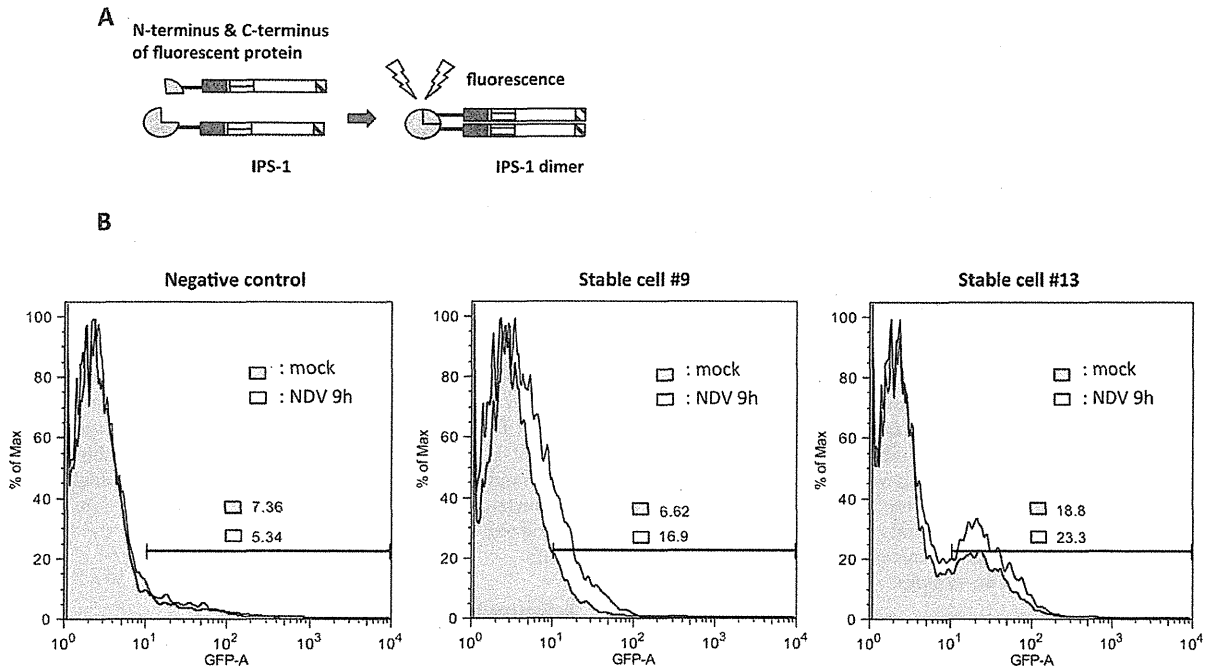

Figure 5. Viral infection induces the molecular oligomer of IPS-1. A. Schematic representation of dimers detection by mKG-tagged IPS-1. B. Flow cytometry plots of control 293T cells and 2 clones stably expressing mKG-tagged IPS-1, #9 and #13. The cells were mock treated or infected with NDV for 9 h. Cells exhibiting fluorescent intensity $>10^1$ were quantified and expressed as % of total cell number.
doi:10.1371/journal.pone.0053578.g005

cDNA Reverse Transcription Kit (Applied Biosystems) was used for cDNA synthesis and mRNA levels were monitored with the Step One plus Real Time PCR system and TaqMan Fast Universal PCR Master Mix (Applied Biosystems). TaqMan primer-probes for human IFNB1, IL-6, IFNA8, and 18 s rRNA were purchased from Applied Biosystems. RNA copy numbers were normalized to that of an internal 18 s rRNA. In the microarray analysis, we used the Genopal microarray system according to the manufacturer's instructions (Mitsubishi Rayon). Biotin-labeled RNA was prepared with a MessageAmp II-Biotin Enhanced kit (Ambion).

Immunoblotting and Antibodies

The polyclonal antibody used to detect human IRF-3 in native PAGE and anti-human IRF-3 polyclonal antibodies for immunostaining were described previously [35]. Other antibodies were obtained from the following sources: Anti-human NF-κB antibody (sc-109), anti-human TRAF6 (sc-8409), and anti-human MFN1 (sc-50330) from Santa Cruz Biotechnology, anti-HA-Tag (6E2) from Cell Signaling, and anti-human Actin (A-1978) from Sigma.

Immunofluorescence Microscopy

For immunofluorescence analysis, cells were fixed with 4% paraformaldehyde for 10 min, permeabilized with acetone: methanol (1:1), and blocked with 5 mg/ml of BSA in PBST (0.04% Teen20 in PBS) for 1hour. Cells were incubated with relevant primary antibodies overnight at 4°C, then incubated with Alexa Fluor-conjugated secondary antibodies (Invitrogen). To label mitochondria, cells were incubated for 30 min at 37°C with MitoTracker Red CMXRos according to the manufacturer's instructions (Molecular Probes). Fluorescence images were obtained by Leica Microsystems AF6500 (Leica).

RNA Interference

The siRNA negative control, targeting TRAF3 and TRAF6 were purchased from Bonac Corporation. The target sequences were: (GCUCAUGGAUGCUGUGCAUdTdT) and (GGAGAAACCUGUUGUGAUUdTdT) for TRAF3 and 6, respectively. Each siRNA was transfected with Lipofectamine 2000 (Invitrogen) according to the manufacturer's instructions. At 48 h post-transfection, cells were harvested, and then subjected to Real Time PCR.

FACS

To examine oligomerization of IPS-1 in cells, we performed bimolecular fluorescence complementation (BiFC) assays using a CoralHue Fluo-Chase kit (Amalgam).

293T cells expressing this construct were washed and harvested with PBS, then subjected to FACS analysis using FACSCanto II (BD Bioscience).

Supporting Information

Figure S1 Microarray analysis of mRNAs induced by oligomerized IPS-1 CARD or IPS-1. HeLa cells stably expressing FK-IPS or FK-IPS CARD were stimulated with AP20187 for the indicated time. Total RNA extracted from these cells was subjected to analysis using a DNA microarray (Genopal, Mitsubishi Rayon) of interferon-stimulated genes and interferon genes. Relative mRNA levels using a control expression as 1.0 are shown.
(PDF)

Figure S2 FK-IPS ΔCARDΔTM forms speckle like aggregates in the cytoplasm. HeLa cells stably expressing FK-IPS ΔCARDΔTM were mock treated or treated with

AP20187 for 3 h and stained with mitoTracker (mitochondria) and anti-HA antibody. Fluorescent microscopic images of FK-IPSΔCARDΔTM and mitochondria are shown.
(PDF)

Figure S3 MFN1 is dispensable for signaling induced by forced oligomerization of IPS-1. MEFs of MFN1−/− or +/+ were transiently transfected with p-125Luc (reporter for IFN-β promoter activity) together with the indicated FK-IPS fusion constructs. Cells were treated with or without AP20187 for 6 h. Relative luciferase activities were determined as described in Materials and Methods. A representative result of at least two independent experiments is shown. Error bars indicate standard error of triplicate samples.
(PDF)

Figure S4 FK-IPS 400–508 can activate IRF-responsive promoter upon oligomerization. HEK 293T cells were transiently transfected with p-55C1BLuc together with the FK or FK-IPS 400–540 constructs. Cells were treated with or without AP20187 for 6 h. Relative luciferase activities were determined as described in Materials and Methods. A representative result of at least two independent experiments is shown. Error bars indicate standard error of triplicate samples.
(PDF)

Figure S5 IPS-1Δ100–500 (mini-MAVS) failed to activate signaling in the absence of endogenous IPS-1. IPS-1−/− or +/+ MEFs were transiently transfected with luciferase reporter plasmid, p-55C1BLuc together with IPS-1(MAVS), IPS-1Δ100–500 (mini-MAVS), or control vector. Relative luciferase activities were determined as described in Materials and Methods. A representative result of at least two independent experiments is shown. Error bars indicate standard error of triplicate samples.
(PDF)

Figure S6 Recruitment of TRAF6 into NP-40 insoluble fraction upon oligomerization of IPS-1. A. Scheme for isolation of soluble and insoluble fractions by differential centrifugation. **B and C.** Immunoblot analysis of soluble/insoluble fractions separated by differential centrifugation. FK-IPS ΔCARD stable cells were cultured for 3 h in the absence or presence of AP. Cell lysates were separated by differential centrifugation. FK-IPS ΔCARD and endogenous MFN1, TRAF6, and actin were detected by immunoblotting.
(PDF)

Figure S7 Involvement of CARD9 in NF-κB dependent pathway. A. HeLa FK-IPS#48 cells were transfected with N.C. siRNA or CARD9 targeted siRNA for 48 h, and the knockdown of CARD9 was analyzed by RT-PCR. **B, C and D.** HeLa FK-IPS#48 cells were transfected with N.C. siRNA or CARD9 targeted siRNA for 48 h, then mock treated or treated with AP20187 for 3 h. Cellular RNA were extracted and analyzed for IFN-β (B), Il-6 (C) or Il-1β (D) mRNA by qPCR. Representative data of at least two independent experiments are shown. Error bars: standard error of triplicated samples. Statistical analyses were conducted with an unpaired t test, with values of $p<0.05$ considered statistically significant. *$p<0.05$.
(PDF)

Acknowledgments

We are grateful to S. Akira for the IPS-1 deficient MEFs, Z. J. Chen for the plasmid constructs, and D. Chan for MFN1 deficient MEFs.

Author Contributions

Conceived and designed the experiments: ST K. Onoguchi K. Onomoto MY TF. Performed the experiments: ST K. Onoguchi K. Onomoto RN FI TKF. Analyzed the data: ST K. Onoguchi K. Onomoto RN KT FI MY HK TF TKF. Wrote the paper: ST K. Onoguchi K. Onomoto RN MY HK TF.

References

1. Yoneyama M, Kikuchi M, Natsukawa T, Shinobu N, Imaizumi T, et al. (2004) The RNA helicase RIG-I has an essential function in double-stranded RNA-induced innate antiviral responses. Nat Immunol 5: 730–737.
2. Yoneyama M, Kikuchi M, Matsumoto K, Imaizumi T, Miyagishi M, et al. (2005) Shared and unique functions of the DExD/H-box helicases RIG-I, MDA5, and LGP2 in antiviral innate immunity. J Immunol 175: 2851–2858.
3. Pichlmair A, Schulz O, Tan CP, Naslund TI, Liljestrom P, et al. (2006) RIG-I-mediated antiviral responses to single-stranded RNA bearing 5′-phosphates. Science 314: 997–1001.
4. Hornung V, Ellegast J, Kim S, Brzozka K, Jung A, et al. (2006) 5′-Triphosphate RNA is the ligand for RIG-I. Science 314: 994–997.
5. Onoguchi K, Yoneyama M, Takemura A, Akira S, Taniguchi T, et al. (2007) Viral infections activate types I and III interferon genes through a common mechanism. J Biol Chem 282: 7576–7581.
6. Sambhara S, Fujita T (2012) Nucleic Acid Sensors and Antiviral Immunity. Austin (TX): Landes Bioscience.
7. Kawai T, Takahashi K, Sato S, Coban C, Kumar H, et al. (2005) IPS-1, an adaptor triggering RIG-I- and Mda5-mediated type I interferon induction. Nat Immunol 6: 981–988.
8. Meylan E, Curran J, Hofmann K, Moradpour D, Binder M, et al. (2005) Cardif is an adaptor protein in the RIG-I antiviral pathway and is targeted by hepatitis C virus. Nature 437: 1167–1172.
9. Seth RB, Sun L, Ea CK, Chen ZJ (2005) Identification and characterization of MAVS, a mitochondrial antiviral signaling protein that activates NF-kappaB and IRF 3. Cell 122: 669–682.
10. Xu LG, Wang YY, Han KJ, Li LY, Zhai Z, et al. (2005) VISA is an adapter protein required for virus-triggered IFN-beta signaling. Mol Cell 19: 727–740.
11. Onoguchi K, Onomoto K, Takamatsu S, Jogi M, Takemura A, et al. (2010) Virus-infection or 5′ppp-RNA activates antiviral signal through redistribution of IPS-1 mediated by MFN1. PLoS Pathog 6: e1001012.
12. Hou F, Sun L, Zheng H, Skaug B, Jiang QX, et al. (2011) MAVS forms functional prion-like aggregates to activate and propagate antiviral innate immune response. Cell 146: 448–461.
13. Li XD, Sun L, Seth RB, Pineda G, Chen ZJ (2005) Hepatitis C virus protease NS3/4A cleaves mitochondrial antiviral signaling protein off the mitochondria to evade innate immunity. Proc Natl Acad Sci U S A 102: 17717–17722.
14. Tang ED, Wang CY (2009) MAVS self-association mediates antiviral innate immune signaling. J Virol 83: 3420–3428.
15. Tang ED, Wang CY (2010) TRAF5 is a downstream target of MAVS in antiviral innate immune signaling. PLoS One 5: e9172.
16. Saha SK, Pietras EM, He JQ, Kang JR, Liu SY, et al. (2006) Regulation of antiviral responses by a direct and specific interaction between TRAF3 and Cardif. EMBO J 25: 3257–3263.
17. Clackson T, Yang W, Rozamus LW, Hatada M, Amara JF, et al. (1998) Redesigning an FKBP-ligand interface to generate chemical dimerizers with novel specificity. Proc Natl Acad Sci U S A 95: 10437–10442.
18. Ouda R, Onomoto K, Takahasi K, Edwards MR, Kato H, et al. (2011) Retinoic acid-inducible gene I-inducible miR-23b inhibits infections by minor group rhinoviruses through down-regulation of the very low density lipoprotein receptor. J Biol Chem 286: 26210–26219.
19. Yoneyama M, Fujita T (2010) Recognition of viral nucleic acids in innate immunity. Rev Med Virol 20: 4–22.
20. Ye H, Arron JR, Lamothe B, Cirilli M, Kobayashi T, et al. (2002) Distinct molecular mechanism for initiating TRAF6 signalling. Nature 418: 443–447.
21. Ueyama T, Kusakabe T, Karasawa S, Kawasaki T, Shimizu A, et al. (2008) Sequential binding of cytosolic Phox complex to phagosomes through regulated adaptor proteins: evaluation using the novel monomeric Kusabira-Green System and live imaging of phagocytosis. J Immunol 181: 629–640.
22. Belgnaoui SM, Paz S, Hiscott J (2011) Orchestrating the interferon antiviral response through the mitochondrial antiviral signaling (MAVS) adapter. Curr Opin Immunol 23: 564–572.
23. Koshiba T (2012) Mitochondrial-mediated antiviral immunity. Biochim Biophys Acta.
24. Lin R, Heylbroeck C, Pitha PM, Hiscott J (1998) Virus-dependent phosphorylation of the IRF-3 transcription factor regulates nuclear translocation, transactivation potential, and proteasome-mediated degradation. Mol Cell Biol 18: 2986–2996.

25. Mao AP, Li S, Zhong B, Li Y, Yan J, et al. (2010) Virus-triggered ubiquitination of TRAF3/6 by cIAP1/2 is essential for induction of interferon-beta (IFN-beta) and cellular antiviral response. J Biol Chem 285: 9470–9476.
26. Paz S, Vilasco M, Arguello M, Sun Q, Lacoste J, et al. (2009) Ubiquitin-regulated recruitment of IkappaB kinase epsilon to the MAVS interferon signaling adapter. Mol Cell Biol 29: 3401–3412.
27. Shirane M, Nakayama KI (2003) Inherent calcineurin inhibitor FKBP38 targets Bcl-2 to mitochondria and inhibits apoptosis. Nat Cell Biol 5: 28–37.
28. Paz S, Vilasco M, Werden SJ, Arguello M, Joseph-Pillai D, et al. (2011) A functional C-terminal TRAF3-binding site in MAVS participates in positive and negative regulation of the IFN antiviral response. Cell Res 21: 895–910.
29. Oganesyan G, Saha SK, Guo B, He JQ, Shahangian A, et al. (2006) Critical role of TRAF3 in the Toll-like receptor-dependent and -independent antiviral response. Nature 439: 208–211.
30. Yoshida R, Takaesu G, Yoshida H, Okamoto F, Yoshioka T, et al. (2008) TRAF6 and MEKK1 play a pivotal role in the RIG-I-like helicase antiviral pathway. J Biol Chem 283: 36211–36220.
31. Poeck H, Bscheider M, Gross O, Finger K, Roth S, et al. (2010) Recognition of RNA virus by RIG-I results in activation of CARD9 and inflammasome signaling for interleukin 1 beta production. Nat Immunol 11: 63–69.
32. Yoneyama M, Suhara W, Fukuhara Y, Fukuda M, Nishida E, et al. (1998) Direct triggering of the type I interferon system by virus infection: activation of a transcription factor complex containing IRF-3 and CBP/p300. EMBO J 17: 1087–1095.
33. Daly C, Reich NC (1993) Double-stranded RNA activates novel factors that bind to the interferon-stimulated response element. Mol Cell Biol 13: 3756–3764.
34. Kumar H, Kawai T, Kato H, Sato S, Takahashi K, et al. (2006) Essential role of IPS-1 in innate immune responses against RNA viruses. J Exp Med 203: 1795–1803.
35. Iwamura T, Yoneyama M, Yamaguchi K, Suhara W, Mori W, et al. (2001) Induction of IRF-3/−7 kinase and NF-kappaB in response to double-stranded RNA and virus infection: common and unique pathways. Genes Cells 6: 375–388.

HEPATOLOGY
Official Journal of the American Association for the Study of Liver Diseases

Hepatitis C Virus NS4B Protein Targets STING and Abrogates RIG-I–Mediated Type I Interferon-Dependent Innate Immunity

Sayuri Nitta,[1*] Naoya Sakamoto,[1,2,6*] Mina Nakagawa,[1,2] Sei Kakinuma,[1,2] Kako Mishima,[1] Akiko Kusano-Kitazume,[1] Kei Kiyohashi,[1] Miyako Murakawa,[1] Yuki Nishimura-Sakurai,[1] Seishin Azuma,[1] Megumi Tasaka-Fujita,[1] Yasuhiro Asahina,[1,2] Mitsutoshi Yoneyama,[3] Takashi Fujita,[4,5] and Mamoru Watanabe[1]

Hepatitis C virus (HCV) infection blocks cellular interferon (IFN)-mediated antiviral signaling through cleavage of Cardif by HCV-NS3/4A serine protease. Like NS3/4A, NS4B protein strongly blocks IFN-β production signaling mediated by retinoic acid–inducible gene I (RIG-I); however, the underlying molecular mechanisms are not well understood. Recently, the stimulator of interferon genes (STING) was identified as an activator of RIG-I signaling. STING possesses a structural homology domain with flaviviral NS4B, which suggests a direct protein-protein interaction. In the present study, we investigated the molecular mechanisms by which NS4B targets RIG-I–induced and STING-mediated IFN-β production signaling. IFN-β promoter reporter assay showed that IFN-β promoter activation induced by RIG-I or Cardif was significantly suppressed by both NS4B and NS3/4A, whereas STING-induced IFN-β activation was suppressed by NS4B but not by NS3/4A, suggesting that NS4B had a distinct point of interaction. Immunostaining showed that STING colocalized with NS4B in the endoplasmic reticulum. Immunoprecipitation and bimolecular fluorescence complementation (BiFC) assays demonstrated that NS4B specifically bound STING. Intriguingly, NS4B expression blocked the protein interaction between STING and Cardif, which is required for robust IFN-β activation. NS4B truncation assays showed that its N terminus, containing the STING homology domain, was necessary for the suppression of IFN-β promoter activation. NS4B suppressed residual IFN-β activation by an NS3/4A-cleaved Cardif (Cardif1-508), suggesting that NS3/4A and NS4B may cooperate in the blockade of IFN-β production. *Conclusion*: NS4B suppresses RIG-I–mediated IFN-β production signaling through a direct protein interaction with STING. Disruption of that interaction may restore cellular antiviral responses and may constitute a novel therapeutic strategy for the eradication of HCV. (HEPATOLOGY 2013;57:46-58)

Type I interferon (IFN) plays a central role in eliminating hepatitis C virus (HCV) both under physiological conditions and when used as a therapeutic intervention.[1-3] In experimental acute-resolving HCV infection in chimpanzees, numerous IFN-related genes are expressed during clinical course of infection.[4] Viruses are recognized by cellular innate immune receptors, such as toll-like receptors, and a family of RIG-I–like receptors, such as retinoic-acid-inducible gene I (RIG-I) and melanoma-differentiation-associated gene 5 (MDA-5); host antiviral responses are then activated, resulting in the

From the [1]Departments of Gastroenterology and Hepatology; [2]Departments of Hepatitis Control, Tokyo Medical and Dental University, Tokyo, Japan; [3]Division of Molecular Immunology, Medical Mycology Research Center, Chiba University, Chiba, Japan; [4]Laboratory of Molecular Genetics, Department of Genetics and Molecular Biology, Institute for Virus Research, Kyoto University, Kyoto, Japan; [5]Laboratory of Molecular Cell Biology, Graduate School of Biostudies, Kyoto University, Kyoto, Japan; and [6]Department of Gastroenterology and Hepatology, Hokkaido University, Hokkaido, Japan.

Received September 16, 2011; accepted July 24, 2012.

BiFC, bimolecular fluorescence complementation; CARD, caspase recruitment domain; DAPI, 4',6-diamidino-2-phenylindole; dsRNA, double-stranded RNA; ER, endoplasmic reticulum; FACL4, fatty acid-CoA ligase, long chain 4; HCV, hepatitis C virus; IFN, interferon; IKKε, IκB kinase ε; IRF-3, interferon-regulatory factor 3; ISRE, interferon-stimulated response element; MAM, mitochondria-associated ER membrane; mKG, monomeric Kusabira-Green; PDI, protein disulphide-isomerase; pIRF-3, phosphorylated IRF3; poly(dA:dT), poly(deoxyadenylic-deoxythymidylic) acid; RIG-I, retinoic acid–inducible gene I; siRNA, small interfering RNA; SOCS, suppressor of cytokine signaling; STAT1, signal transducer and activator of transcription protein-1; STING, stimulator of interferon genes; TBK1, TANK binding kinase 1.

**These authors contributed equally to this work.*

production of cytokines such as type I and type III IFNs.[5] RIG-I is activated through recognition of short double-strand RNA (dsRNA) or triphosphate at the 5′ end of dsRNA as pathogen-associated molecular patterns,[6,7] forming a homo-oligomer that binds with the caspase recruitment domain (CARD) of Cardif (also known as MAVS, VISA, or IPS-1).[8-11] Cardif subsequently recruits TANK binding kinase 1 (TBK1) and IκB kinase ϵ (IKKϵ) kinases, which catalyze phosphorylation and activation of IFN regulatory factor-3 (IRF-3).[12] Activation of TBK1 and IKKϵ results in the phosphorylation of IRF-3 or IRF-7, translocation to the nucleus, and induction of IFN-β mRNA transcription.

Several HCV proteins can block host cellular antiviral responses. HCV core protein blocks IFN signaling by interacting with signal transducer and activator of transcription protein-1 (STAT1).[13] The core protein also induces expression of suppressor of cytokine signaling-1 (SOCS1) and SOCS3, and blocks Janus kinase–STAT signaling.[14,15] A well-elucidated immune evasion strategy of HCV involves NS3/4A serine protease and its ability to inhibit host IFN signal pathways. Gale and colleagues[11,16,17] revealed that NS3/4A protease cleaves Cardif at Cys-508 resulting in dislocation of Cardif from mitochondria, and blocks downstream signaling of IFN-β production. On the other hand, Baril et al.[18] reported that Cardif was still able to form a homo-oligomer and to activate downstream IFN production signaling despite delocalization from the mitochondria. These reports suggest that homo-oligomerization of Cardif, and not mitochondrial anchorage, is essential for the activation of downstream IFN signaling and that other virus-derived molecules may cooperate with NS3/4A to abrogate the signaling of IFN production.

We reported previously that HCV-NS4B, as well as NS3/4A, inhibited RIG-I and Cardif-mediated interferon-stimulated response element (ISRE) activation, while TBK1- and IKKϵ-mediated ISRE activation were not suppressed.[19] These results indicate that NS4B suppresses IFN production signaling by targeting Cardif or other unknown signaling molecules between the level of Cardif and TBK1/IKKϵ.

Recently, a stimulator of interferon genes (STING, also known as MITA/ERIS/MPYS/TMEM173) was identified as a positive regulator of RIG-I–mediated IFN-β signaling.[20-23] STING is a 42-kDa protein localized predominantly in the endoplasmic reticulum (ER) that binds RIG-I, Cardif, TBK1, and IKKϵ. STING is thought to act as a scaffold for Cardif/TBK1/IRF-3 complex upon viral infection.[22] It has been reported that NS4B of yellow fever virus, which is a member of the flaviviridae family of viruses, inhibits STING activation probably through a direct molecular interaction.[24] These reports have led us postulate that HCV-NS4B may also inhibit RIG-I dependent IFN signaling through association with STING.

In the present study, we further investigated the molecular mechanisms by which HCV-NS4B protein inhibits RIG-I–mediated IFN expression signaling. We demonstrated that HCV-NS4B specifically binds STING, blocks the molecular interaction between STING and Cardif, and suppresses the RIG-I–like receptor–induced activation of IFN-β production signaling.

Materials and Methods

Plasmids. The ΔRIG-I and RIG-IKA plasmids express constitutively active and inactive RIG-I, respectively.[5] Full-length Cardif (Cardif) and CARD-truncated Cardif (ΔCARD) plasmids were provided by J. Tschopp.[11] Plasmids expressing STING were provided by G. N. Barber.[20] Plasmids expressing HCV NS3/4A, NS4B, and truncated NS4B have been described.[25] Plasmid pIFNβ-Fluc was provided by R. Lin.[26]

Cell Culture. HEK293T and Huh7 cells were maintained in Dulbecco's modified minimal essential medium (Sigma) supplemented with 2 mM L-glutamine and 10% fetal calf serum at 37°C with 5% CO_2.

HCV Replicon Constructs and HCV-JFH1 Cell Culture. An HCV subgenomic replicon plasmid, pRep-Feo, expressed fusion protein of firefly luciferase and neomycin phosphotransferase.[27,28] Huh7 cells were transfected by Rep-Feo RNA, cultured in the presence of 500 μg/mL of G418, and a cell line that stably expressed Feo replicon was established. For HCV cell culture, the HCV-JFH1 strain was used.[29,30]

Antibodies. Antibodies used were anti–IRF-3 (FL-425, Santa Cruz Biotechnology), anti-HA (Invitrogen), anti-myc (Invitrogen), mouse anti-PDI (Abcam),

Address reprint requests to: Naoya Sakamoto, M.D., Ph.D., Department of Gastroenterology and Hepatology, Hokkaido University, Kita15, Nishi8, Kita-ku, Sapporo, Hokkaido, 060-0808, Japan. E-mail: nsakamoto.gast@tmd.ac.jp; fax (81)-11-706-8036.

View this article online at wileyonlinelibrary.com.

DOI 10.1002/hep.26017

Potential conflict of interest: Nothing to report.

Additional Supporting Information may be found in the online version of this article.

rabbit anti-PDI (Enzo Life Science), anti-Flag (Sigma Aldrich), anti-Cardif (Enzo Life Science), anti-phospho–IRF-3 (Ser396, Millipore), anti-monomeric Kusabira-Green C- or N-terminal fragment (MBL), and anti-FACL4 (Abgent).

Luciferase Reporter Assay. IFN-β reporter assays were performed as described.[19,31] The plasmids pIFN-β-Fluc and pRL-CMV were cotransfected with NS3/4A or NS4B, and ΔRIG-I, Cardif, STING or poly(deoxyadenylic-deoxythymidylic) acid [poly(dA:dT)] (Invivogen). RIG-IKA, ΔCARD, and pcDNA3.1, respectively, were used as controls. Luciferase assays were performed 24 hours after transfection by using a 1420 Multilabel Counter (ARVO MX PerkinElmer) and Dual Luciferase Assay System (Promega). Assays were performed in triplicate, and the results are expressed as the mean ± SD.

Immunoblotting. Preparation of total cell lysates was performed as described.[19,28] Protein was separated using NuPAGE 4%-12% Bis/Tris gels (Invitrogen) and blotted onto an Immobilon polyvinylidene difluoride membrane. The membrane was immunoblotted with primary followed by secondary antibody, and protein was detected by chemiluminescence.

Immunoprecipitation Assay. HEK-293T or Huh7 cells were transfected with plasmids as indicated. Twenty-four hours after transfection, cellular proteins were harvested and immunoprecipitation assays were performed using an Immunoprecipitation Kit according to the manufacturer's protocol (Roche Applied Science). The immunoprecipitated proteins were analyzed by immunoblotting.

Indirect Immunofluorescence Assay. Cells seeded onto tissue culture chamber slides were transfected with plasmids as indicated. Twenty-four hours after transfection, the cells were fixed with cold acetone and incubated with primary antibody and subsequently with Alexa488- or Alexa568-labeled secondary antibodies. Mitochondria were stained by MitoTracker (Invitrogen). Cells were visualized using a confocal laser microscope (Fluoview FV10, Olympus).

BiFC Assay. Expression plasmids of NS4B, Cardif, or STING that was fused with N- or C-terminally truncated monomeric Kusabira-Green (mKG) were constructed by inserting polymerase chain reaction–amplified fragments encoding NS4B, Cardif, or STING, respectively, inserted into fragmented mKG vector (Coral Hue Fluo-Chase Kit; MBL). HEK293T cells were transfected with a complementary pair of mKG fusion plasmids. Twenty-four hours after transfection, fluorescence-positive cells were detected and counted by flow cytometry, or observed by confocal laser microscopy.

Small Interfering RNA Assay. Nucleotide sequences of STING-targeted small interfering RNAs (siRNAs) were as follows: (1) 5′-gcaacagcatctatgagcttctggagaac-3′, (2) 5′- gtgcagtgagccagcggctgtatattctc;-3′, (3) 5′-gctggcat ggtcatattacatcggatatc-3′.[22] Stealth RNAi Negative Control Duplex (Medium GC Duplex, Invitrogen) was used. Forty-eight hours after siRNA transfection, expression levels of STING were detected by immunoblotting.

Statistical Analyses. Statistical analyses were performed using unpaired, two-tailed Student t test. $P < 0.05$ were considered to be statistically significant.

Results

NS4B Suppressed RIG-I, Cardif, and STING-Mediated Activation of IFN-β Expression Signaling. First, we performed a reporter assay using a luciferase reporter plasmid regulated by native IFN-β promoter. Consistent with our previous study,[19] overexpression of NS4B, as well as NS3/4A, inhibited the IFN-β promoter activation that was induced by ΔRIG-I and Cardif, respectively (Fig. 1A). We next studied whether NS4B targets STING and inhibits RIG-I pathway–mediated activation of IFN-β production. Expression of NS4B protein significantly suppressed STING-mediated activation of the IFN-β promoter reporter, whereas expression of NS3/4A showed no effect on STING-induced IFN-β promoter activity (Fig. 1A). To study whether NS4B blocks the STING-mediated DNA-sensing pathway, we performed a reporter assay using a luciferase reporter plasmid cotransfection with poly(dA:dT), which is a synthetic analog of B-DNA and has been reported to induce STING-mediated IFN-β production and NS4B. NS4B significantly blocked poly(dA:dT)-induced IFN-β promoter activation, suggesting that NS4B may block STING signaling in the DNA-sensing pathway (Fig. 1A).

Activation of RIG-I signaling induces phosphorylation of IRF-3, which is a hallmark of IRF-3 activation.[32] Thus, we examined the effects of NS3/4A and NS4B expression on phosphorylation of IRF-3 by immunoblotting analysis. As shown in Fig. 1B, overexpression of ΔRIG-I, Cardif, or STING in HEK293T cells increased levels of phosphorylated IRF-3 (pIRF-3). Expression of NS4B impaired the IRF-3 phosphorylation that was induced by ΔRIG-I, Cardif, or STING. NS3/4A also blocked production of pIRF-3 induced by ΔRIG-I or Cardif. Intriguingly, NS3/4A did not block STING-induced pIRF-3 production. These results demonstrate that both NS3/4A and

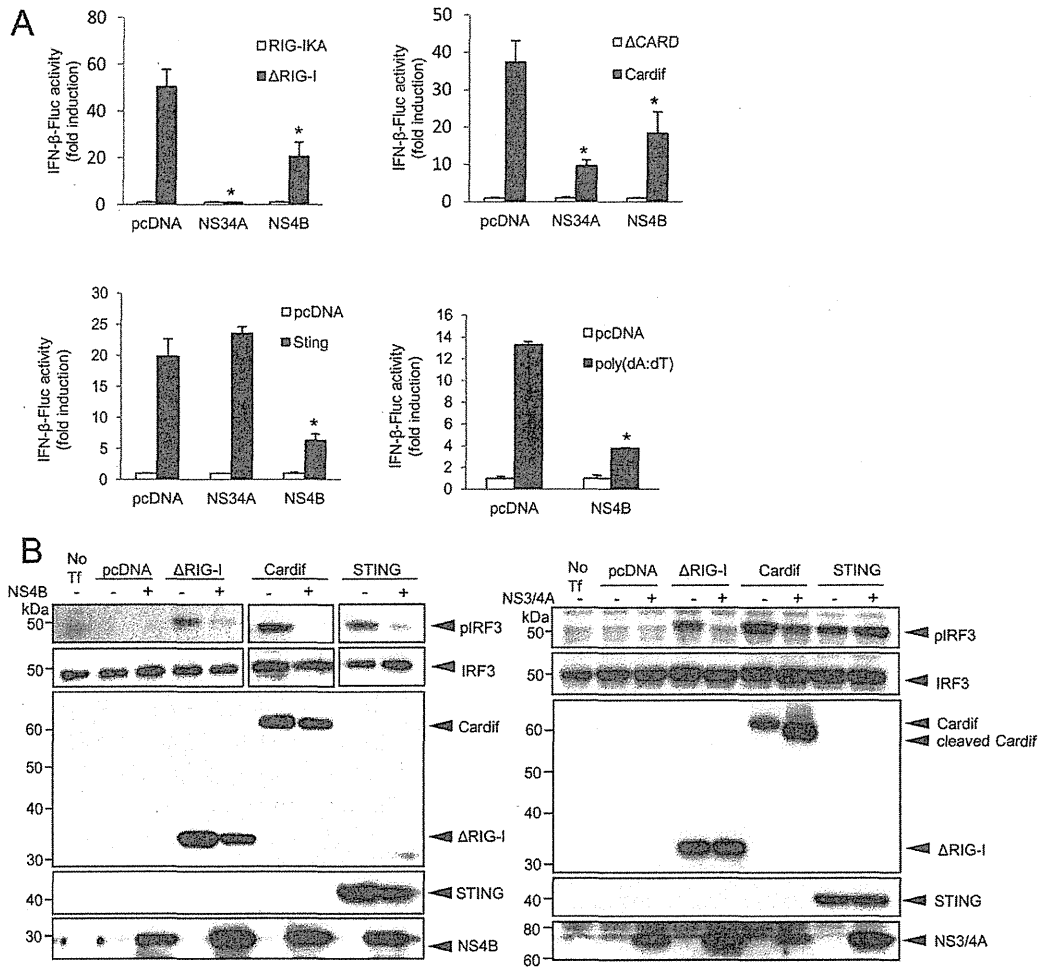

Fig. 1. NS4B suppressed IFN-β signaling mediated by RIG-I, Cardif, or STING. (A) Plasmids expressing ΔRIG-I, Cardif, or STING or poly(dA:dT) as well as NS3/4A or NS4B were cotransfected with pIFN-β-Fluc and pRL-CMV into HEK293T cells. After 24 hours, dual luciferase assays were performed. Plasmids expressing RIG-IKA, ΔCARD, or an empty plasmid (pcDNA) were used as a corresponding negative control. The experiments were performed more than three times and yielded consistent results. The *y* axis indicates relative IFN-β-Fluc activity. Assays were performed in triplicate and error bars indicate mean ± SD. $^*P < 0.05$. (B) HEK293T cells were cotransfected with indicated plasmids. On the day after transfection, the cells were lysed and immunoblot analyses were performed. No Tf, transfection-negative controls. pIRF-3 and IRF-3, phosphorylated and total IRF-3, respectively.

NS4B suppress RIG-I–mediated IFN-β production, but they do so by targeting different molecules in the signaling pathway.

Subcellular Localization of NS4B, Cardif, and STING. We next studied the subcellular localization of NS4B following its overexpression and measured the colocalization of NS4B with Cardif and STING in both HEK293T cells and Huh7 cells by indirect immunofluorescence microscopy. NS4B was localized predominantly in the ER, which is consistent with previous reports[33] (Fig. 2A). Cardif was localized in mitochondria but did not colocalize with the ER-resident host protein disulphide-isomerase (PDI). Interestingly, Cardif and NS4B colocalized partly at the boundary of the two proteins, although their original localization was different (Fig. 2A,C). STING was localized predominantly in the ER[20,21] (Fig. 2B,D). STING colocalized partly with Cardif, which is consistent with a previous report by Ishikawa and Barber[20] (Fig. 2B,D). In cells cotransfected with NS4B and STING expression plasmids, NS4B colocalized precisely with STING (Fig. 2B,D). To examine the region of NS4B-STING interaction, we next observed the two proteins by performing staining for them along with mitochondria-associated ER membrane (MAM), which is a physical association with mitochondria[34] and has been reported the site of Cardif-STING association.[24] Both NS4B and STING were adjacent to and partially colocalized

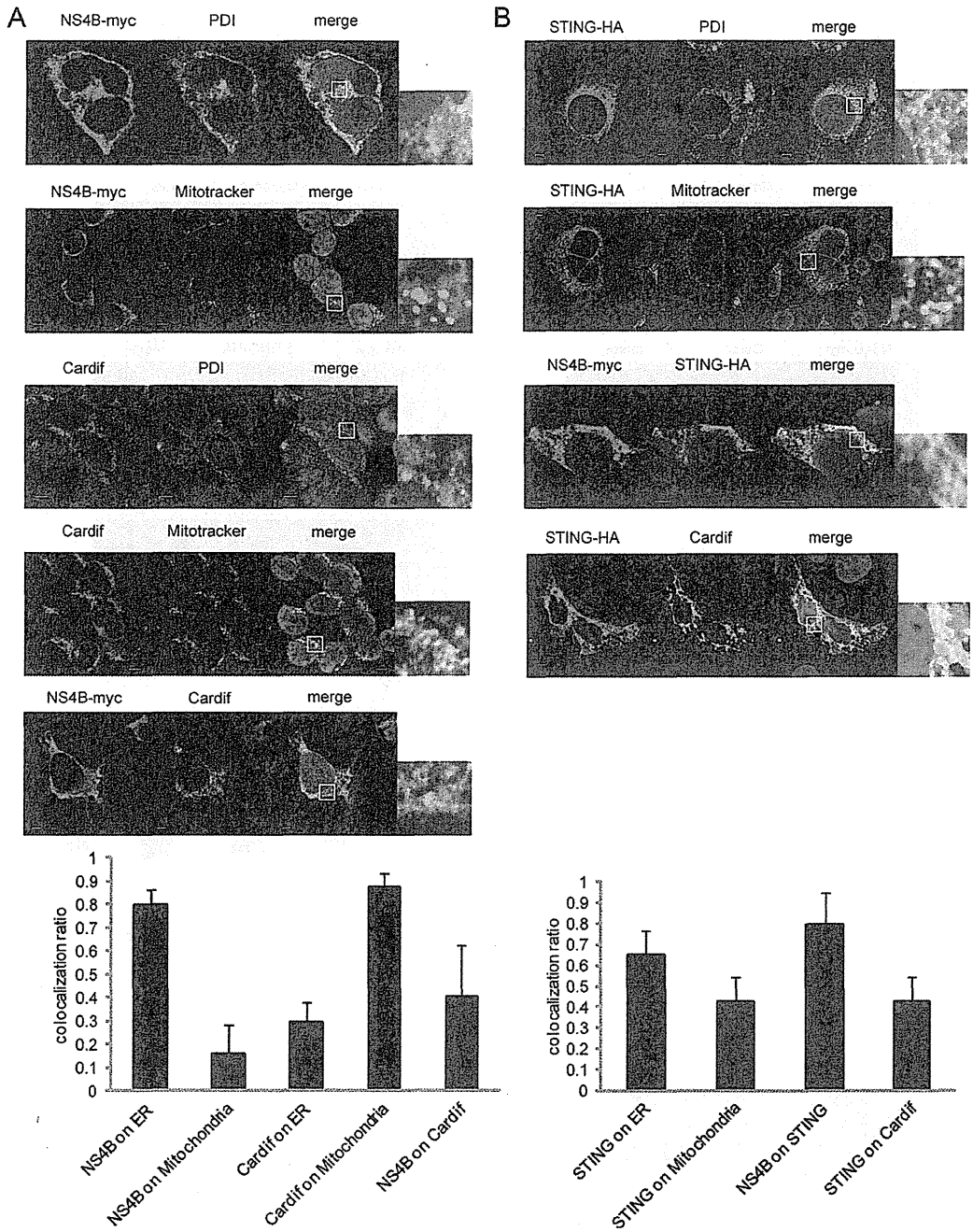

Fig. 2. Subcellular localization of NS4B, Cardif, and STING. (A-D) Subcellular localization of NS4B, Cardif, and STING in 293T (A,C) and Huh7 (B,D) cells. (A,C) NS4B-myc (first, second, and fifth panels of A and third panel of C) was transfected, and 24 hours later the cells were fixed and immunostained with anti-myc. In the third, fourth, and fifth panels of A, and the first and second panels of C, endogenous Cardif was detected with anti-Cardif antibody. ER was immunostained with anti-PDI antibody (first and third panels of A and first panel of C). Mitochondria were stained using Mitotracker (second and fourth panels of A and second panel of C). Nuclei were stained with 4',6-diamidino-2-phenylindole (DAPI). (B,D) STING-HA (all panels) and NS4B-myc (third panels) were transfected, and after 24 hours the cells were fixed and immunostained with anti-HA or anti-myc, respectively. In the fourth panels, endogenous Cardif was detected with anti-Cardif antibody. ER was immunostained with anti-PDI antibody (first panels). Mitochondria were stained using Mitotracker (second panels). Nuclei were stained with DAPI. (E) NS4B-myc and STING-HA were transfected into Huh7 cells and after 24 hours the cells were fixed and immunostained with anti-HA, anti-myc, and anti-FACL4 (MAM) antibody. Cells were visualized by confocal microscopy. Scale bars indicate 5 μm. In each microscopic image, the grade of protein colocalization in a single cell was quantified and is shown in the graphs at the bottom of each panel. Values are shown as the average colocalization ratio in 8 cells. Error bars indicate the mean + SD.

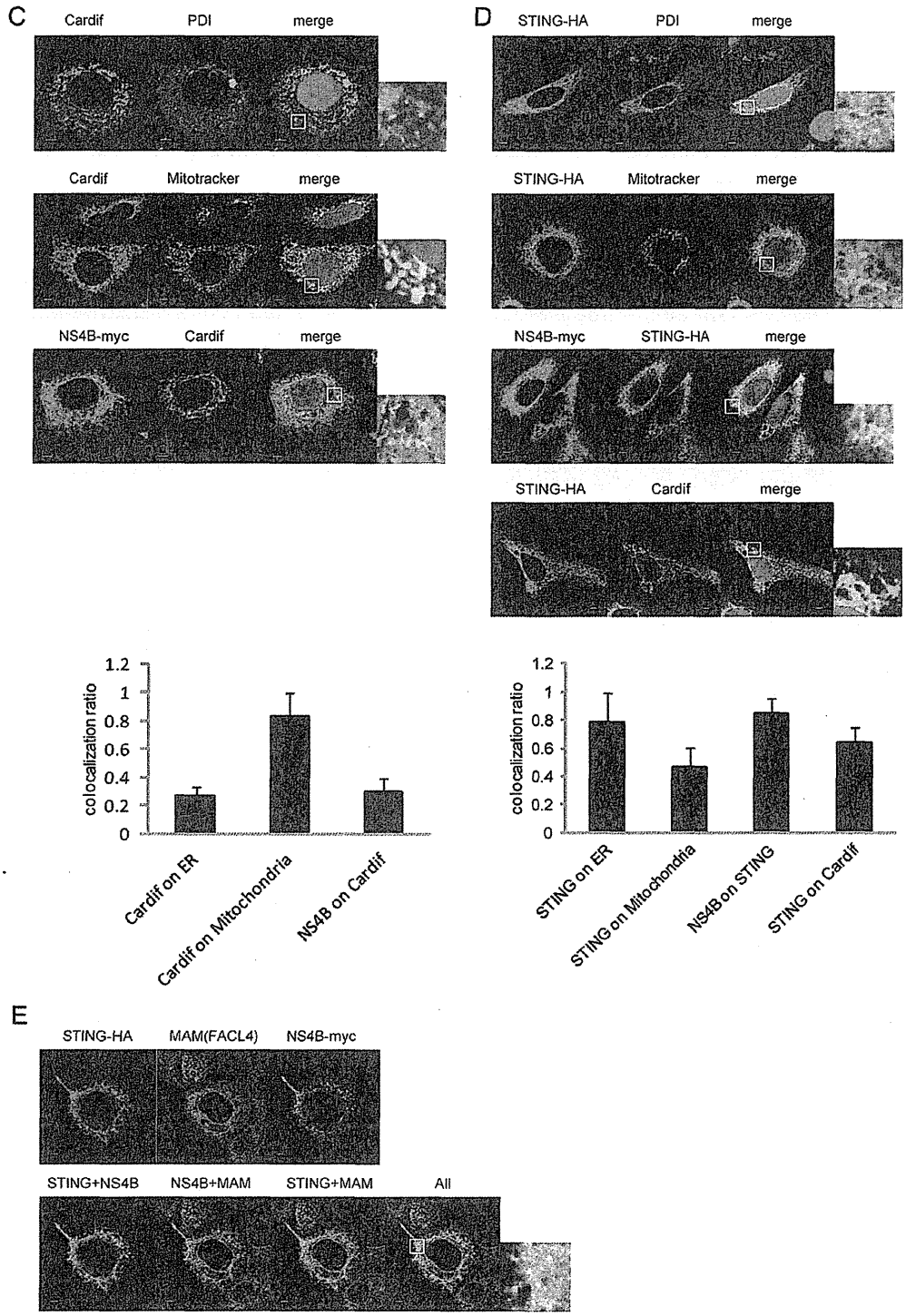

Fig. 2. Continued

with fatty acid-CoA ligase long chain 4 (FACL4), which is a MAM marker protein[35,36] (Fig. 2E). These findings suggest that NS4B might interact with STING on MAM more strongly than with Cardif.

Protein-Protein Interaction Between NS4B, Cardif, and STING. Knowing that NS4B was colocalized strongly with STING and only partly with Cardif, we next analyzed direct protein-protein interactions

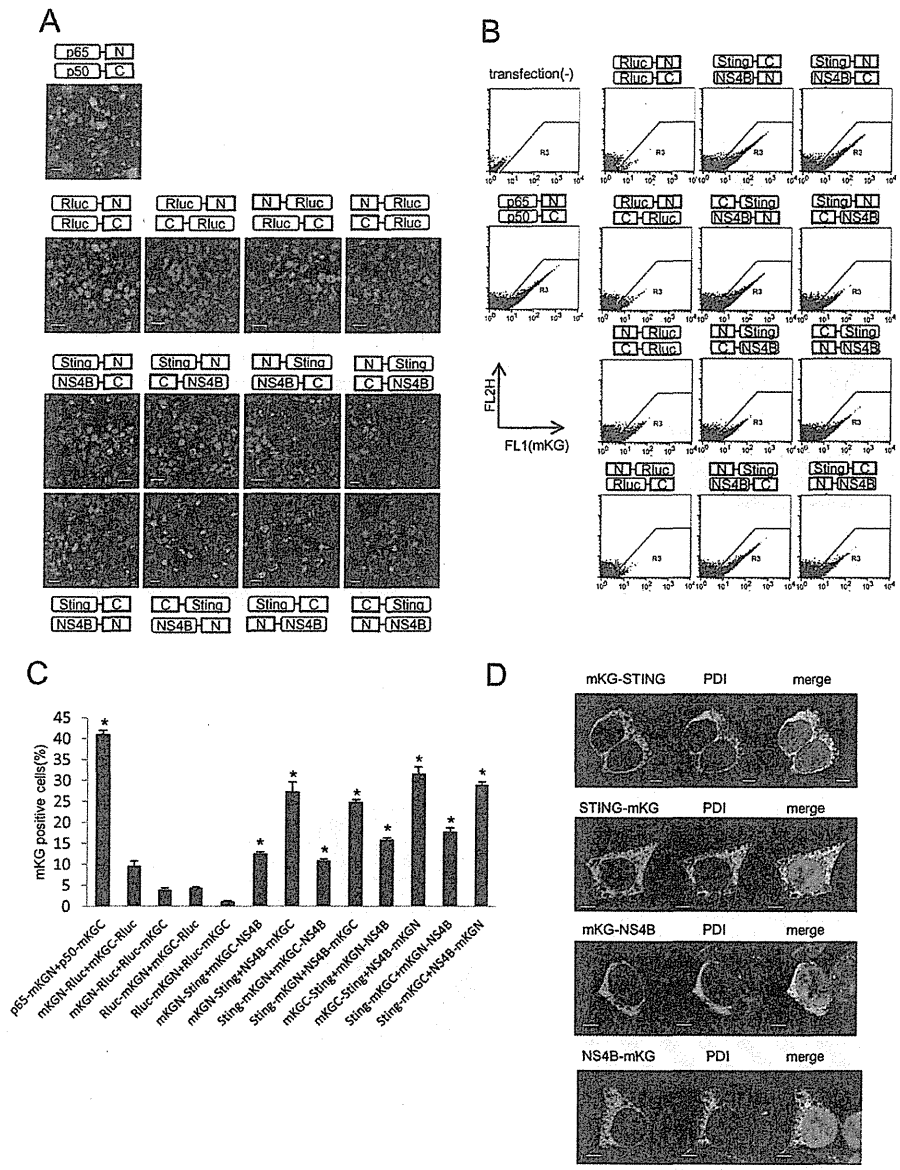

Fig. 3. BiFC assays of STING and NS4B. The complementary pairs of N- or C-terminally mKG-fused NS4B and STING expression plasmids were cotransfected in HEK293T cells. After 24 hours, the cells were fixed and observed by confocal microscopy (A) or subjected to flow cytometry to measure mKG-emitted fluorescence (BiFC signal) and to count BiFC signal-positive cells (B,C). Plasmids expressing p65-mKGN and p50-mKGC individually were used as a BiFC-positive control and plasmids expressing N- or C-terminally mKG fused Rluc were used as a negative control. The letters N and C denote complimentary N- and C-terminal fragments of mKG, respectively. Assays were performed in triplicate and error bars indicate the mean ± SD. Scale bars indicate 10 μm (A). *$P < 0.05$ compared with corresponding negative controls. (D) Plasmids expressing mKG fragment-fused STING or NS4B were transfected in HEK293T cells. After 24 hours, the cells were fixed and immunostained with anti-mKG and anti-PDI (ER) antibody. Nuclei were stained with DAPI. Cells were observed by confocal microscopy. Scale bars = 5 μm.

between NS4B, Cardif, and STING. To detect those interactions in living cells, we performed BiFC assays.[37,38] We constructed NS4B, Cardif, and STING expression plasmids that were N- or C-terminally fused with truncated mKG proteins, respectively. First, we cotransfected several different pairs of NS4B and STING expression plasmids that were fused with complementary pairs of N- or C-terminally truncated mKG. Strong fluorescence by mKG complexes (BiFC signal) was detected in all pairs of cotransfections, suggesting significant molecular interaction (Fig. 3A). In flow cytometry, all pairs of NS4B- and STING-mKG fusion proteins were positive for strong BiFC signal (Fig. 3B). The percentages of cells positive for BiFC signal were significantly higher in STING-mKG and NS4B-mKG fusion complexes than in corresponding controls (Fig. 3C). These results demonstrate that HCV-NS4B and STING proteins interact with each other strongly and specifically in cells. Fluorescence microscopy indicated that N- and C-terminal fusion of mKG onto NS4B and STING did not affect subcellular localization (Fig. 3D).

We next studied the molecular interaction between NS4B and Cardif by BiFC assay using NS4B and Cardif fusion plasmids that were tagged with complementary pairs of truncated mKG. Weak fluorescence was detected in cells transfected with the pairs N-Cardif and NS4B-C, N-Cardif and C-NS4B, C-Cardif and

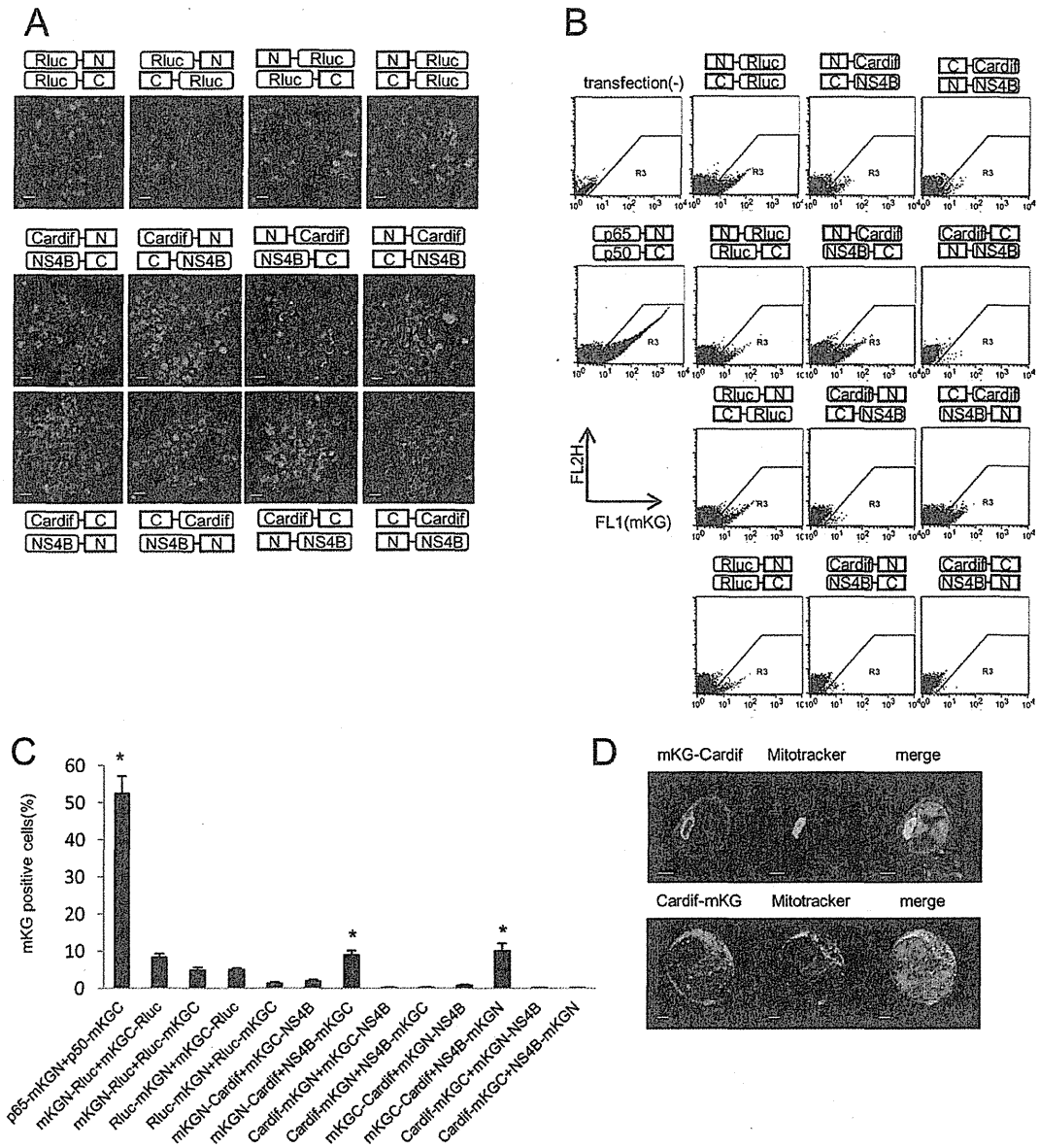

Fig. 4. BiFC assays of Cardif and NS4B. The complementary pairs of N- or C-terminally mKG-fused NS4B and Cardif expression plasmids were cotransfected in HEK293T cells. After 24 hours, the cells were fixed and observed by confocal microscopy (A) or subjected to flow cytometry to measure mKG-emitted fluorescence (BiFC signal) and to count BiFC signal-positive cells (B,C). Plasmids expressing p65-mKGN and p50-mKGC individually were used as a BiFC-positive control and plasmids expressing N- or C-terminally mKG-fused Rluc were used as a negative control. The letters N and C denote complimentary N- and C-terminal fragments of mKG, respectively. Assays were performed in triplicate, and error bars indicate the mean ± SD. Scale bars indicate 10 μm (A). *$P < 0.05$ compared with corresponding negative controls. (D) Plasmids expressing mKG fragment-fused STING or NS4B were transfected in HEK293T cells. After 24 hours, the cells were fixed and immunostained with anti-mKG antibody. Mitochondria were stained using Mitotracker, and nuclei were stained with DAPI. Cells were observed by confocal microscopy. Scale bars = 5 μm.

NS4B-N, and C-Cardif and N-NS4B (Fig. 4A,B). The percentage of cells positive for BiFC signal increased with the combination of N-Cardif and NS4B-C, and C-Cardif and NS4B-N (Fig. 4C). Fluorescence microscopy indicated that mKG-Cardif, but not Cardif-mKG, was partially colocalized with mitochondria, possibly due to disruption of mitochondria anchor domain by C-terminal fusion with mKG (Fig. 4D). These results indicate the lack of significant molecular interactions between NS4B and Cardif.

Binding of NS4B to STING Blocks Molecular Interaction Between Cardif and STING. It has been reported that STING binds Cardif directly.[20,22] Thus, we hypothesized that NS4B, through a competitive

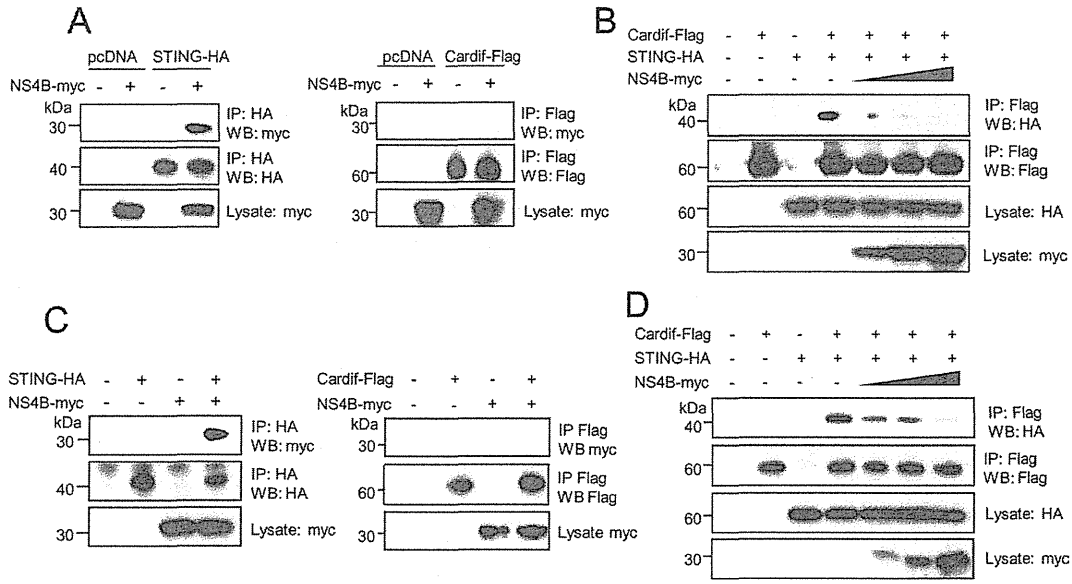

Fig. 5. Binding of NS4B to STING blocks molecular the interaction between Cardif and STING. (A,C) NS4B expression plasmid was cotransfected with STING or Cardif expression plasmid into HEK293T cells (A) or Huh7 cells (C). After 24 hours, cell lysates were subjected to immunoprecipitation using anti-HA or anti-Flag and were immunoblotted with anti-myc. (B,D) Cardif and STING expression plasmids were cotransfected with various amounts of NS4B plasmid in HEK293T cells (B) or Huh7 cells (D). After 24 hours, cells lysates were subjected to immunoprecipitation using anti-Flag and were immunoblotted with anti-HA.

interaction with STING, may hinder the direct molecular interaction between Cardif and STING. To verify this hypothesis, we performed immunoprecipitation assays. First, we transfected plasmids that expressed NS4B and Cardif, or NS4B and STING, in HEK293T cells or Huh7 cells, and performed immunoprecipitation. NS4B strongly bound to STING in both HEK293T cells and Huh7 cells, suggesting specific molecular interactions, whereas NS4B and Cardif did not show any obvious interaction (Fig. 5A,C). Consistent with previous reports, STING and Cardif showed significant interaction (Fig. 5B,D). Interestingly, those interactions were decreased by coexpression of NS4B, depending on its input amount, and finally blocked completely in both HEK293T and Huh7 cells (Fig. 5B,D). Collectively, the results above demonstrate that NS4B disrupts the interaction between Cardif and STING possibly through competitive binding to STING.

Effects on HCV Infection and Replication Levels by STING Knockdown and NS4B Overexpression. We next studied the impact of STING-mediated IFN production and its regulation by NS4B on HCV infection and cellular replication. First, we transfected three STING-targeted siRNAs into Huh7/Feo cells (Fig. 6A). As shown in Fig. 6B, STING knockdown cells conferred significantly higher permissibility to HCV replication. We next transfected HCV-JFH1 RNA into Huh7 cells that were transiently transfected with NS4B. As shown in Fig. 6C, HCV core protein expression was significantly higher in NS4B-overexpressed cells. Furthermore, HCV replication was increased significantly in Huh7/Feo cells overexpressing NS4B (Fig. 6D). Taken together, the results above demonstrate that STING and NS4B may negatively or positively regulate cellular permissiveness to HCV replication.

The N-terminal Domain of NS4B Is Essential for Suppressing IFN-β Promoter Activity Mediated by RIG-I, Cardif, and STING. It has been reported that the N-terminal domain of several forms of flaviviral NS4B shows structural homology with STING.[24] We therefore investigated whether the STING homology domain in NS4B is responsible for suppression of IFN-β production. We constructed two truncated NS4B expression plasmids, which covered the N terminus (NS4Bt1-84, amino acids 1 through 84) containing the STING homology domain and the C terminus (NS4Bt85-261, amino acids 85 through 261), respectively (Fig. 7A). Immunoblotting showed that NS4Bt1-84 and NS4Bt85-261 yielded protein bands of ~9 kDa and ~20 kDa, respectively. Aberrant bands in the truncated NS4B may be due to alternative posttranslational processing. HEK293T cells were transfected with ΔRIG-I, Cardif, or STING, and NS3/4A or the truncated NS4B, along with IFN-β-Fluc plasmid, and a reporter assay was performed. NS4Bt1-84 significantly suppressed RIG-I, Cardif, and STING-

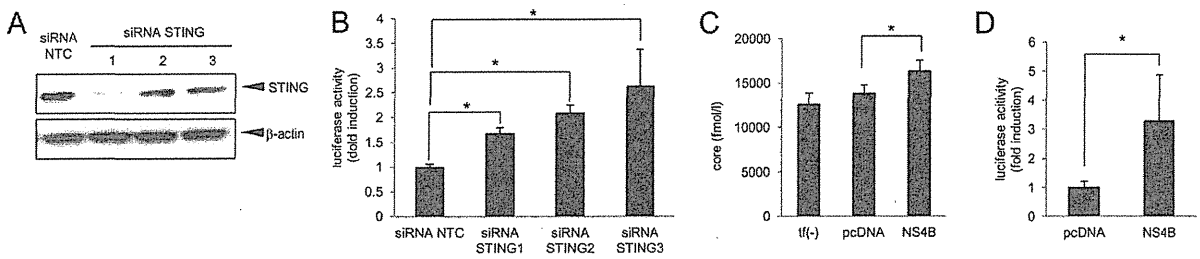

Fig. 6. Effects on HCV replication levels by STING knockdown and NS4B overexpression. (A) Effects of siRNA knockdown of STING by siRNA. Huh7 cells were transfected with STING-targeted siRNAs (siRNA STING-1, -2, and -3, respectively) or negative control siRNA (siRNA NTC). Seventy-two hours after transfection, cells were harvested and expression levels of STING protein were detected by immunoblotting. (B) Huh7 cells expressing HCV-Feo subgenomic replicon (Huh7/Feo)[27,28] were transfected with STING-targeted siRNAs or negative control siRNA. Seventy-two hours after transfection, cells were harvested, and internal luciferase activities were measured. The *y* axis indicates luciferase activity shown as a ratio of transfection-negative control. Assays were performed in triplicate, and error bars indicate the mean + SD. $*P < 0.05$ compared with corresponding negative controls. (C) Empty plasmid or plasmid expressing NS4B was transfected into Huh7 cells. After 24 hours, HCV-JFH1 RNA was transfected into these cells. Seventy-two hours after virus transfection, HCV core antigen levels in culture medium were measured. Assays were performed in triplicate, and error bars indicate the mean + SD. $*P < 0.05$ compared with corresponding negative controls. tf(−), transfection-negative control. (D) Huh7 cells expressing HCV-Feo replicon (Huh7/Feo)[27,28] were transfected with NS4B expressing plasmid or empty plasmid (pcDNA). Forty-eight hours after transfection, internal luciferase activities were measured. The *y* axis indicates luciferase activity shown as a ratio of the transfection-negative control. Assays were performed in triplicate, and error bars indicate the mean + SD. $*P < 0.05$ compared with corresponding negative controls.

induced IFN-β promoter activity, whereas NS4Bt85-261 did not (Fig. 7B). These results suggest that the N-terminal domain of NS4B is responsible for association with STING. Fluorescent microscopy indicated that both NS4Bt1-84 and NS4Bt85-26 colocalized with ER and STING (Fig. 7C).

NS4B Suppresses IFN Production Signaling Cooperatively with NS3/4A. It has been reported that

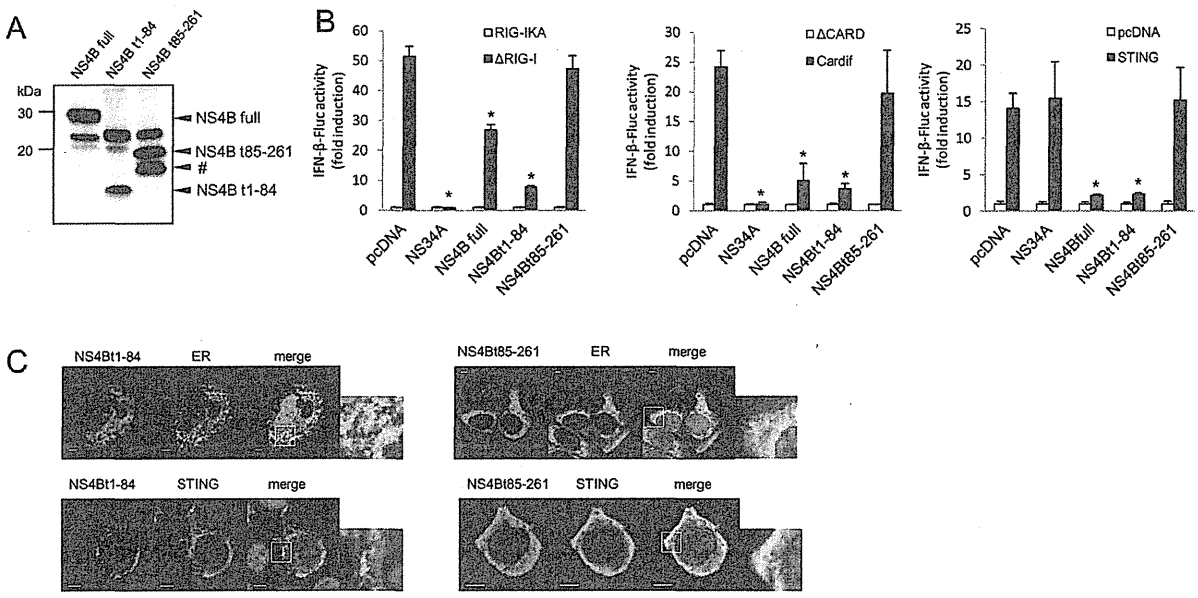

Fig. 7. The N-terminal domain of NS4B is essential for suppressing IFN-β promoter activity induced by RIG-I, Cardif, or STING. (A) Immunoblotting of NS4B and truncated NS4B, NS4B t1-84, and NS4Bt85-216. HEK293T cells were transfected with NS4B or truncated NS4B. After 24 hours, the cells were lysed and immunoblot assays were performed. The band indicated by the pound sign (#) is a truncated NS4B, probably generated via alternative posttranslational processing. (B) Plasmids expressing ΔRIG-I, Cardif, or STING as well as NS3/4A or the indicated truncated form of NS4B were cotransfected with pIFN-β-Fluc and pRL-CMV in HEK293T cells. Dual luciferase assays were performed 24 hours after transfection. Plasmids expressing RIG-IKA, ΔCARD, or pcDNA were used as negative controls. The *y* axis indicates IFN-β-Fluc activity shown as relative values. Assays were performed in triplicate, and error bars indicate the mean ± SD. $*P < 0.05$ compared with corresponding negative controls. (C) Plasmids expressing NS4Bt1-84-myc of NS4Bt85-261-myc were transfected with or without plasmids expressing HA-STING in HEK293T cells. After 24 hours, the cells were fixed and immunostained. Nuclei were stained with DAPI. Cells were observed by confocal microscopy. Scale bars indicate 5 μm.

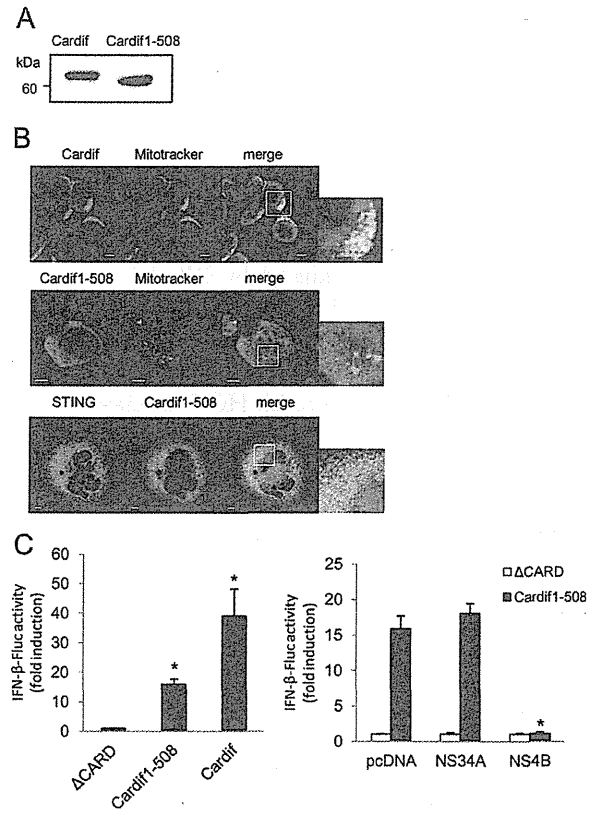

Fig. 8. NS4B suppressed IFN-β production pathway independently of and cooperatively with NS3/4A. (A) Immunoblotting of Cardif and truncated Cardif (Cardif1-508). HEK293T cells were transfected with Cardif or truncated Cardif (Cardif1-508). After 24 hours, the cells were lysed and immunoblot assays were performed. (B) Subcellular localization of Cardif and truncated Cardif (Cardif1-508). HEK293T cells were immunostained with anti-Cardif antibody or HEK293T cells were transfected with myc-tagged truncated Cardif (Cardif1-508-myc), and after 24 hours the cells were immunostained with anti-myc. Mitochondria were stained with Mitotracker (red) and nuclei were stained with DAPI (blue). Plasmid expressing myc-tagged truncated Cardif (Cardif1-508) and plasmid expressing HA-tagged STING were transfected into HEK293T cells. The cells were immunostained with anti-myc and anti-HA antibodies and analyzed by confocal laser microscopy. Scale bars = 10 μm. (C) Plasmids expressing Cardif or truncated Cardif (Cardif1-508) and pIFN-β-Fluc and pRL-CMV were transfected with or without plasmid expressing NS3/4A or NS4B into HEK293T cells as indicated. Dual luciferase assays were performed 24 hours after transfection. Plasmid expressing ΔCARD or pcDNA was used as a negative control. The *y* axis indicates IFN-β-Fluc activity shown as relative values. Assays were performed in triplicate, and error bars indicate the mean ± SD. $^*P < 0.05$.

HCV NS3/4A serine protease cleaves Cardif between Cys-508 and His-509, releases Cardif from the mitochondrial membrane, and blocks RIG-I–induced IFN-β production. We next assessed whether NS4B suppresses IFN-β production in the presence of Cardif cleaved by NS3/4A protease (Cardif1-508, Fig. 8A). The truncation of Cardif–C-terminal residue abolished mitochondrial localization but still colocalized with STING (Fig. 8B). The reporter assay showed that Cardif1-508 induced weak IFN-β activation. Interestingly, NS4B completely blocked the residual function of the Cardif1-508 protein to activate IFN-β expression, suggesting an additive effect of NS3/4A and NS4B on the RIG-I–activating pathway (Fig. 8C).

Discussion

It has been reported that viruses, including HCV, target IFN signaling to establish persistent replication in host cells.[39] We have reported that NS4B blocks the transcriptional activation of ISRE induced by overexpression of RIG-I and Cardif, but not by TBK1 or IKKϵ.[19] In the present study, we have shown that NS4B directly and specifically binds STING, an ER-residing scaffolding protein of Cardif and TBK1 and an inducer of IFN-β production (Figs. 3 and 5), and blocked the interaction between STING and Cardif (Fig. 5B,D) resulting in strong suppression of RIG-I–mediated phosphorylation of IRF-3 and expressional induction of IFN-β (Fig. 1). Furthermore, HCV replication was increased by knockdown of STING or overexpression of NS4B (Fig. 6). Taken together, our results demonstrate that HCV-NS4B strongly blocks virus-induced, RIG-I–mediated activation of IFN-β production signaling through targeting STING, which constitutes a novel mechanism of viral evasion from innate immune responses and establishment of persistent viral replication.

Our results also showed that the effects of NS4B on the RIG-I signaling were independent of NS3/4A-mediated cleavage of Cardif. Reporter assays showed that a cleaved form of Cardif (Cardif1-508) partially retained activity for the induction of IFN-β promoter activation. The residual IFN-β promoter activation was suppressed almost completely by NS4B but not by NS3/4A (Fig. 8C). These findings show that there are at least two mechanisms by which HCV can abrogate RIG-I–mediated IFN production signaling to accomplish abrogation of cellular antiviral responses.

NS4B and STING are ER proteins,[20,21,40] whereas Cardif is localized on the outer mitochondrial membrane.[9] Consistent with those reports, our immunostaining experiments demonstrated that most NS4B protein colocalized with STING (Fig. 2), and their association was localized on MAM (Fig. 2E). In addition to the significant colocalization of STING and NS4B, STING partially colocalized with Cardif at the boundary region of the two proteins (Fig. 2B). Furthermore, immunoprecipitation experiments showed that overexpression of NS4B completely blocked the interaction of STING with Cardif (Fig. 5B). Ishikawa et al.[24] reported

that STING could associate with Cardif by MAM interaction. Castanier et al.[41] reported that Cardif-STING interaction was enhanced in cells with elongated mitochondria. In addition, Horner et al.[42,43] observed NS3/4A targeting of MAM-anchored synapse and cleavage of Cardif at MAM but not in mitochondria. These results led us to speculate that interaction between STING and Cardif was enhanced by altering their subcellular localization during viral infection and that NS4B inhibits Cardif activation by interfering with the association between STING and Cardif on MAM-like NS3/4A behavior against host innate immunity.

HCV-NS4B is an ER-localized 27-kDa protein with several functions in the HCV life cycle. Cellular expression of NS4B induces convolution of the ER membrane and formation of a membranous web that harbors HCV replicase complex.[44,45] NS4B also has RNA-binding capacity.[46] In addition, several point mutations of NS4B were found to alter viral replication activity.[33,46,47] The studies above indicate that NS4B provides an important protein-protein or protein-RNA interaction platform within the HCV replication complex and is essential for viral RNA replication. However, there are few reports on the involvement of NS4B with antiviral immune responses. Consistent with our previous study, Moriyama et al.[48] reported that NS4B partially inhibited dsRNA-induced but not TRIF-induced activation of IFN-β. In NS4B-expressing cells, IFN-α induced activation of STAT1 was suppressed.[49] The present study has demonstrated that NS4B functions against the host IFN response, such that NS4B directly interacts with STING and suppresses downstream signaling, resulting in the induction of IFN production.

STING contains a domain homologous to the N terminus of NS4B derived from several flaviviruses, including HCV. In our previous NS4B truncation assay, the NS4B N-terminal domain (amino acids 1-110) was important for suppression of RIG-I–induced IFN-β expression.[19] Consistent with these results, N-terminally truncated NS4B (NS4Bt1-84) significantly suppressed STING and Cardif-induced IFN-β promoter activation, whereas the C terminus of NS4B (NS4Bt85-261) did not (Fig. 7). These results reinforce our hypothesis that NS4B binds STING at its homology domain and blocks the ability of STING to induce IFN-β production.

A small molecule inhibitor of NS4B has been developed and is under preliminary clinical trials.[50] Einav et al.[51] identified clemizole hydrochloride, an H1 histamine receptor antagonist, as an inhibitor of the RNA-binding function of NS4B and HCV RNA replication. A phase 1B clinical trial of clemizole in hepatitis C patients has been completed.[52] Other two NS4B inhibitors which are a compound of amiloride analog and anguizole are under preclinical development.[53,54] The possibility remains that such NS4B inhibitors may suppress HCV replication partly through inhibiting the ability of NS4B to suppress IFN-β production and restore cellular antiviral responses.

In conclusion, IFN production signaling induced by HCV infection and mediated by RIG-I is suppressed by NS4B through a direct interaction with STING. These virus-host interactions help to elucidate the mechanisms of persistent HCV infection and constitute a potential target to block HCV infection.

Acknowledgment: The authors are indebted to J. Tcshopp for providing Cardif, ΔCARD, and CARD and to G. N. Barber for the STING plasmids. This study was supported by grants from the Ministry of Education, Culture, Sports, Science and Technology, Japan; the Japan Society for the Promotion of Science; Ministry of Health, Labour and Welfare, Japan; and the Japan Health Sciences Foundation.

References

1. Samuel CE. Antiviral actions of interferons. Clin Microbiol Rev 2001; 14:778-809.
2. Taniguchi T, Takaoka A. The interferon-alpha/beta system in antiviral responses: a multimodal machinery of gene regulation by the IRF family of transcription factors. Curr Opin Immunol 2002;14:111-116.
3. Sakamoto N, Watanabe M. New therapeutic approaches to hepatitis C virus. J Gastroenterol 2009;44:643-649.
4. Bigger CB, Brasky KM, Lanford RE. DNA microarray analysis of chimpanzee liver during acute resolving hepatitis C virus infection. J Virol 2001;75:7059-7066.
5. Yoneyama M, Kikuchi M, Natsukawa T, Shinobu N, Imaizumi T, Miyagishi M, et al. The RNA helicase RIG-I has an essential function in duoble-stranded RNA-induced innate antiviral responses. Nat Immunol 2004;5:730-737.
6. Hornung V, Ellegast J, Kim S, Brzozka K, Jung A, Kato H, et al. 5'-Triphosphate RNA is the ligand for RIG-I. Science 2006;314:994-997.
7. Takahasi K, Yoneyama M, Nishihori T, Hirai R, Kumeta H, Narita R, et al. Nonself RNA-sensing mechanism of RIG-I helicase and activation of antiviral immune responses. Mol Cell 2008;29:428-440.
8. Kawai T. IPS-1, an adaptor triggering RIG-I- and Mda5-mediated type I interferon induction. Nat Immunol 2005;6:981-988.
9. Seth RB, Sun L, Ea CK, Chen ZJ. Identification and characterization of MAVS, a mitochondrial antiviral signaling protein that activates NF-κB and IRF 3. Cell 2005;122:669-682.
10. Xu LG. VISA is an adapter protein required for virus-triggered IFN-β signaling. Mol Cell 2005;19:727-740.
11. Meylan E, Curran J, Hofmann K, Moradpour D, Binder M, Bartenschlager R, et al. Cardif is an adaptor protein in the RIG-I antiviral pathway and is targeted by hepatitis C virus. Nature 2005;437: 1167-1172.
12. Yoneyama M, Suhara W, Fukuhara Y, Fukuda M, Nishida E, Fujita T. Direct triggering of the type I interferon system by virus infection: activation of a transcription factor complex containing IRF-3 and CBP/p300. EMBO J 1998;17:1087-1095.

13. Lin W, Kim SS, Yeung E, Kamegaya Y, Blackard JT, Kim KA, et al. Hepatitis C virus core protein blocks interferon signaling by interaction with the STAT1 SH2 domain. J Virol 2006;80:9226-9235.
14. Suda G, Sakamoto N, Itsui Y, Nakagawa M, Tasaka-Fujita M, Funaoka Y, et al. IL-6-mediated intersubgenotypic variation of interferon sensitivity in hepatitis C virus genotype 2a/2b chimeric clones. Virology 2010;407:80-90.
15. Funaoka Y, Sakamoto N, Suda G, Itsui Y, Nakagawa M, Kakinuma S, et al. Analysis of interferon signaling by infectious hepatitis C virus clones with substitutions of core amino acids 70 and 91. J Virol 2011; 85:5986-5994.
16. Loo YM, Owen DM, Li K, Erickson AK, Johnson CL, Fish PM, et al. Viral and therapeutic control of IFN-beta promoter stimulator 1 during hepatitis C virus infection. Proc Natl Acad Sci U S A 2006;103:6001-6006.
17. Li X-D, Sun L, Seth RB, Pineda G, Chen ZJ. Hepatitis C virus protease NS3/4A cleaves mitochondrial antiviral signaling protein off the mitochondria to evade innate immunity. Proc Natl Acad Sci U S A 2005; 102:17717-17722.
18. Baril M, Racine M-E, Penin F, Lamarre D. MAVS Dimer Is a Crucial Signaling Component of Innate Immunity and the Target of Hepatitis C Virus NS3/4A Protease. J. Virol. 2009;83:1299-1311.
19. Tasaka M, Sakamoto N, Itakura Y, Nakagawa M, Itsui Y, Sekine-Osajima Y, et al. Hepatitis C virus non-structural proteins responsible for suppression of the RIG-I/Cardif-induced interferon response. J Gen Virol 2007;88:3323-3333.
20. Ishikawa H, Barber GN. STING is an endoplasmic reticulum adaptor that facilitates innate immune signalling. Nature 2008;455:674-678.
21. Sun W, Li Y, Chen L, Chen H, You F, Zhou X, et al. ERIS, an endoplasmic reticulum IFN stimulator, activates innate immune signaling through dimerization. Proc Natl Acad Sci U S A 2009;106:8653-8658.
22. Zhong B, Yang Y, Li S, Wang YY, Li Y, Diao F, et al. The adaptor protein MITA links virus-sensing receptors to IRF3 transcription factor activation. Immunity 2008;29:538-550.
23. Jin L. MPYS, a novel membrane tetraspanner, is associated with major histocompatibility complex class II and mediates transduction of apoptotic signals. Mol Cell Biol 2008;28:5014-5026.
24. Ishikawa H, Ma Z, Barber GN. STING regulates intracellular DNA-mediated, type I interferon-dependent innate immunity. Nature 2009; 461:788-792.
25. Yanagi M, Purcell RH, Emerson SU, Bukh J. Transcripts from a single full-length cDNA clone of hepatitis C virus are infectious when directly trasfected into the liver of a chimpanzee. Proc Natl Acad Sci U S A 1997;94:8738-8743.
26. Lin R, Lacoste J, Nakhaei P, Sun Q, Yang L, Paz S, et al. Dissociation of a MAVS/IPS-1/VISA/Cardif-IKKepsilon molecular complex from the mitochondrial outer membrane by hepatitis C virus NS3-4A proteolytic cleavage. J Virol 2006;80:6072-6083.
27. Yokota T, Sakamoto N, Enomoto N, Tanabe Y, Miyagishi M, Maekawa S, et al. Inhibition of intracellular hepatitis C virus replication by synthetic and vector-derived small interfering RNAs. EMBO Rep 2003;4:602-608.
28. Tanabe Y, Sakamoto N, Enomoto N, Kurosaki M, Ueda E, Maekawa S, et al. Synergistic inhibition of intracellular hepatitis C virus replication by combination of ribavirin and interferon- alpha. J Infect Dis 2004;189:1129-1139.
29. Wakita T, Pietschmann T, Kato T, Date T, Miyamoto M, Zhao Z, et al. Production of infectious hepatitis C virus in tissue culture from a cloned viral genome. Nat Med 2005;11:791-796.
30. Lindenbach BD, Evans MJ, Syder AJ, Wolk B, Tellinghuisen TL, Liu CC, et al. Complete replication of hepatitis C virus in cell culture. Science 2005;309:623-626.
31. Nakagawa M, Sakamoto N, Enomoto N, Tanabe Y, Kanazawa N, Koyama T, et al. Specific inhibition of hepatitis C virus replication by cyclosporin A. Biochem Biophys Res Commun 2004;313:42-47.
32. Yamashiro T, Sakamoto N, Kurosaki M, Kanazawa N, Tanabe Y, Nakagawa M, et al. Negative regulation of intracellular hepatitis C virus replication by interferon regulatory factor 3. J Gastroenterol 2006;41:750-757.
33. Lindstrom H, Lundin M, Haggstrom S, Persson MA. Mutations of the hepatitis C virus protein NS4B on either side of the ER membrane affect the efficiency of subgenomic replicons. Virus Res 2006;121: 169-178.
34. Hayashi T, Rizzuto R, Hajnoczky G, Su TP. MAM: more than just a housekeeper. Trends Cell Biol 2009;19:81-88.
35. Lewin TM, Van Horn CG, Krisans SK, Coleman RA. Rat liver acyl-CoA synthetase 4 is a peripheral-membrane protein located in two distinct subcellular organelles, peroxisomes, and mitochondrial-associated membrane. Arch Biochem Biophys 2002;404:263-270.
36. Simmen T, Aslan JE, Blagoveshchenskaya AD, Thomas L, Wan L, Xiang Y, et al. PACS-2 controls endoplasmic reticulum-mitochondria communication and Bid-mediated apoptosis. EMBO J 2005;24:717-729.
37. Kerppola TK. Design and implementation of bimolecular fluorescence complementation (BiFC) assays for the visualization of protein interactions in living cells. Nat Protoc 2006;1:1278-1286.
38. Kerppola TK. Bimolecular fluorescence complementation (BiFC) analysis as a probe of protein interactions in living cells. Annu Rev Biophys 2008;37:465-487.
39. Kato H. Differential roles of MDA5 and RIG-I helicases in the recognition of RNA viruses. Nature 2006;441:101-105.
40. Saitoh T, Fujita N, Hayashi T, Takahara K, Satoh T, Lee H, et al. Atg9a controls dsDNA-driven dynamic translocation of STING and the innate immune response. Proc Natl Acad Sci U S A 2009;106: 20842-20846.
41. Castanier C, Garcin D, Vazquez A, Arnoult D. Mitochondrial dynamics regulate the RIG-I-like receptor antiviral pathway. EMBO Rep 2009;11:133-138.
42. Horner SM, Liu HM, Park HS, Briley J, Gale M. Mitochondrial-associated endoplasmic reticulum membranes (MAM) form innate immune synapses and are targeted by hepatitis C virus. Proc Natl Acad Sci U S A 2011;108:14590-14595.
43. Horner SM, Park HS, Gale M Jr. Control of innate immune signaling and membrane targeting by the hepatitis C virus NS3/4A protease are governed by the NS3 helix α0. J Virol 2012;86:3112-3120.
44. Egger D, Wolk B, Gosert R, Bianchi L, Blum HE, Moradpour D, et al. Expression of Hepatitis C virus proteins induces distinct membrane alterations including a candidate viral replication complex. J Virol 2002;76:5974-5984.
45. Gretton SN, Taylor AI, McLauchlan J. Mobility of the hepatitis C virus NS4B protein on the endoplasmic reticulum membrane and membrane-associated foci. J Gen Virol 2005;86:1415-1421.
46. Einav S, Elazar M, Danieli T, Glenn JS. A nucleotide binding motif in hepatitis C virus (HCV) NS4B mediates HCV RNA replication. J Virol 2004;78:11288-11295.
47. Elazar M, Liu P, Rice CM, Glenn JS. An N-terminal amphipathic helix in hepatitis C virus (HCV) NS4B mediates membrane association, correct localization of replication complex proteins, and HCV RNA replication. J Virol 2004;78:11393-11400.
48. Moriyama M, Kato N, Otsuka M, Shao RX, Taniguchi H, Kawabe T, et al. Interferon-beta is activated by hepatitis C virus NS5B and inhibited by NS4A, NS4B, and NS5A. Hepatol Int 2007;1:302-310.
49. Xu J, Liu S, Xu Y, Tien P, Gao G. Identification of the nonstructural protein 4B of hepatitis C virus as a factor that inhibits the antiviral activity of interferon-alpha. Virus Res 2009;141:55-62.
50. Hofmann WP, Zeuzem S. A new standard of care for the treatment of chronic HCV infection. Nat Rev. Gastroenterol Hepatol 2011;8: 257-264.
51. Einav S, Gerber D, Bryson PD, Sklan EH, Elazar M, Maerkl SJ, et al. Discovery of a hepatitis C target and its pharmacological inhibitors by microfluidic affinity analysis. Nat Biotech 2008;26:1019-1027.
52. Rai R, Deval J. New opportunities in anti-hepatitis C virus drug discovery: targeting NS4B. Antiviral Res 2011;90:93-101.
53. Cho NJ, Dvory-Sobol H, Lee C, Cho SJ, Bryson P, Masek M, et al. Identification of a class of HCV inhibitors directed against the nonstructural protein NS4B. Sci Transl Med 2010;2:15ra16.
54. Bryson PD, Cho NJ, Einav S, Lee C, Tai V, Bechtel J, et al. A small molecule inhibits HCV replication and alters NS4B's subcellular distribution. Antiviral Res 2010;87:1-8.

Critical Role of an Antiviral Stress Granule Containing RIG-I and PKR in Viral Detection and Innate Immunity

Koji Onomoto[1,2,9¤], Michihiko Jogi[1,3,4], Ji-Seung Yoo[1,3], Ryo Narita[1], Shiho Morimoto[1], Azumi Takemura[1], Suryaprakash Sambhara[5], Atushi Kawaguchi[6,7], Suguru Osari[6], Kyosuke Nagata[6], Tomoh Matsumiya[8], Hideo Namiki[9], Mitsutoshi Yoneyama[4,10]*, Takashi Fujita[1,3]*

1 Laboratory of Molecular Genetics, Institute for Virus Research, Kyoto University, Kyoto, Japan, **2** Research Institute for Science and Engineering, Waseda University, Tokyo, Japan, **3** Laboratory of Molecular Cell Biology, Graduate School of Biostudies, Kyoto University, Kyoto, Japan, **4** Division of Molecular Immunology, Medical Mycology Research Center, Chiba University, Chuo-ku, Chiba, Japan, **5** Influenza Division, Centers for Disease Control and Prevention, Atlanta, Georgia, United States of America, **6** Department of Infection Biology, Faculty of Medicine and Graduate School of Comprehensive Human Sciences, University of Tsukuba, Tsukuba, Japan, **7** Kitasato Institute for Life Sciences, Kitasato University, Tokyo, Japan, **8** Department of Vascular Biology, Institute of Brain Science, Graduate School of Medicine, Hirosaki University, Aomori, Japan, **9** Graduate School of Science and Engineering, Waseda University, Tokyo, Japan, **10** PRESTO, Japan Science and Technology Agency, Honcho Kawaguchi, Saitama, Japan

Abstract

Retinoic acid inducible gene I (RIG-I)-like receptors (RLRs) function as cytoplasmic sensors for viral RNA to initiate antiviral responses including type I interferon (IFN) production. It has been unclear how RIG-I encounters and senses viral RNA. To address this issue, we examined intracellular localization of RIG-I in response to viral infection using newly generated anti-RIG-I antibody. Immunohistochemical analysis revealed that RLRs localized in virus-induced granules containing stress granule (SG) markers together with viral RNA and antiviral proteins. Because of similarity in morphology and components, we termed these aggregates antiviral stress granules (avSGs). Influenza A virus (IAV) deficient in non-structural protein 1 (NS1) efficiently generated avSGs as well as IFN, however IAV encoding NS1 produced little. Inhibition of avSGs formation by removal of either the SG component or double-stranded RNA (dsRNA)-dependent protein kinase (PKR) resulted in diminished IFN production and concomitant enhancement of viral replication. Furthermore, we observed that transfection of dsRNA resulted in IFN production in an avSGs-dependent manner. These results strongly suggest that the avSG is the locus for non-self RNA sensing and the orchestration of multiple proteins is critical in the triggering of antiviral responses.

Citation: Onomoto K, Jogi M, Yoo J-S, Narita R, Morimoto S, et al. (2012) Critical Role of an Antiviral Stress Granule Containing RIG-I and PKR in Viral Detection and Innate Immunity. PLoS ONE 7(8): e43031. doi:10.1371/journal.pone.0043031

Editor: Akio Kanai, Keio University, Japan

Received April 11, 2012; **Accepted** July 16, 2012; **Published** August 13, 2012

Funding: The Ministry of Education, Culture, Sports, Science and Technology in Japan (Innovative Areas "RNA regulation" (No.20112009), Scientific Research "A", and Research Activity Start-up) (http://www.mext.go.jp/english/), the Ministry of Health, Labour and Welfare of Japan (http://www.mhlw.go.jp/english/index.html), the PRESTO Japan Science and Technology Agency (http://www.jst.go.jp/kisoken/presto/index_e.html), the Uehara Memorial Foundation (http://www.ueharazaidan.com/), the Mochida Memorial Foundation for Medical and Pharmaceutical Research (http://www.mochida.co.jp/zaidan/), the Takaeda Science Foundation (http://www.takeda-sci.or.jp/index.html), the Naito Foundation (http://www.naito-f.or.jp/), and Nippon Boehringer Ingelheim (http://www.boehringer-ingelheim.co.jp/com/Home/index.jsp). The funders had no role in study design, data collection and analysis, decision to publish, or preparation of the manuscript.

Competing Interests: The authors have the following competing interests: This study was partly funded by Nippon Boehringer Ingelheim. There are no patents, products in development or marketed products to declare. This does not alter the authors' adherence to all the PLoS ONE policies on sharing data and materials, as detailed online in the guide for authors.

* E-mail: myoneyam@faculty.chiba-u.jp (MY); tfujita@virus.kyoto-u.ac.jp (TF)

¤ Current address: Division of Molecular Immunology, Medical Mycology Research Center, Chiba University, Chuo-ku, Chiba, Japan

Introduction

Type I and III interferons (IFNs) are cytokines with strong antiviral activity [1,2]. Upon the binding of IFNs with their cognate receptor complexes, an intracellular signal is activated resulting in the activation of transcription factors, IFN stimulated gene factor 3, heterotrimer of signal transducer and activator of transcription (STAT)1, STAT2, and IFN regulatory factor (IRF)-9, and STAT1 homodimer. These factors induce the activation of hundreds of interferon stimulated genes (ISGs). Some of the ISG products act as antiviral proteins and participate in the blockade of viral replication. The level of double-stranded (ds) RNA-dependent protein kinase (PKR) is enhanced by IFN treatment, however catalytic activity of PKR requires dsRNA. When IFN-treated cells are infected by virus, dsRNA, produced as a by-product of viral replication, activates PKR, and the activated PKR inactivates eukaryotic translation initiation factor (eIF) 2á by phosphorylation [3]. Another antiviral protein 2′–5′ oligoadenylate synthetase (OAS) is also induced to express by IFN. Catalytic activity of OAS requires dsRNA and virus infection activates OAS to produce 2′–5′ A. 2′–5′ A then activates cellular RNase L, and viral RNA is degraded [1]. Although, the "dsRNA-activated inhibition" model is widely accepted, IFN-treated and virus-infected cells do not necessarily undergo suicide, as conventional IFN bioassays have demonstrated IFN-induced survival of infected cells [4]. To explain these phenomena, it has been hypothesized that viral transcription/translation takes place in a specific subcellular compartment, thus the blocking of translation and the degradation

of RNA by these antiviral proteins little affect host metabolism. However, no one has yet demonstrated such a compartment.

IFNs are not normally produced at biologically significant levels. Most types of mammalian cells are capable of producing IFN upon viral infection. Viral replication is sensed by cytoplasmic non-self RNA sensors; RIG-I, melanoma differentiation-associated gene 5 (MDA5), and laboratory of genetics and physiology 2 (LGP2), which are collectively termed RLRs, to initiate the cascade of events leading to the activation of transcription factors, IRF-3/-7 and nuclear factor-êB (NF-êB), then the activation of IFN genes [5–9]. Thus, the primary function of the IFN system is to sense non-self RNA and to eradicate the invading RNA, which includes RNA derived from the replication of DNA viruses [10,11]. Although genetic evidence shows that RLR is critical for detecting viral RNA in the cytoplasm, its specific distribution has been unknown.

In this report, we investigated the cellular localization of RIG-I in Influenza A Virus -infected cells. We discovered that viral infection or the transfection of viral RNA causes RIG-I to form granular aggregates containing stress granule markers, which we term antiviral stress granules (avSGs). Our analyses revealed that avSGs are critical for signaling to activate the IFN gene, suggesting that the avSG serves as a platform for the sensing of non-self RNA by RLRs. Furthermore, because the granule also recruits PKR, OAS and RNase L, it is strongly suggested to be the compartment where some antiviral proteins inhibit viral replication.

Results

Infection of NS1-deficient IAV Produces Granules Containing RIG-I

We generated an anti-RIG-I antibody, which specifically detects RIG-I by immunostaining and immunoblotting (Figure S1) (Materials and Methods) [12]. To observe the cellular distribution of RIG-I, cells were infected with two types of IAV, the wild type (WT) and ÄNS1 which lacks the gene for non-structural protein 1 (NS1), a potent inhibitor of IFN production [13]. WT IAV replication was detectable at 3 h after infection as a nuclear accumulation of viral nucleocapsid protein (NP) (Figure 1A). Later in the infection (9–12 h), NP, presumably as a complex with viral genomic RNA [14], translocated to the cytoplasm. RIG-I was dispersed in uninfected cells and WT IAV infection did not cause any change in its distribution. On the other hand, in cells infected with IAVÄNS1, NP accumulated in the nucleus at 6 h post-infection, however only a fraction of NP translocated to the cytoplasm at 9–12 h (Figure 1B). Unlike WT IAV, the NP of IAVÄNS1 exhibited a speckle-like distribution in the cytoplasm. Notably, formation of this RIG-I-containing speckle strongly correlates with activation of RIG-I-mediated signal activation as judged by nuclear localization (Figure 1C) and dimerization of IRF-3 and concomitant enhanced production of ISGs, such as RLRs and STAT1 (Data not shown). Indeed, the ratio of cells with IAV- and IAVÄNS1-induced nuclear IRF-3 was 2.7% and 33.7%, respectively, and cells containing RIG-I speckles together with nuclear IRF-3 were 0.0% (IAV) and 72.2% (IAVÄNS1).

IAVÄNS1-induced Granules Contain Both Stress Granule Marker and Anti-viral Proteins

We characterized the nature of these speckles by using various antibodies and found that interestingly, RIG-I exhibited co-localization with NP (83.5%) and a stress granule (SG) marker, T-cell restricted intracellular antigen-related protein (TIAR) (97.1%) at 9 h (Figure 1B). Other SG markers are similarly recruited to the granules produced by IAVÄNS1: Ras-GAP SH3 domain-binding protein (G3BP) (97.6% colocalized with RIG-I), eIF3 (99.8% colocalized with G3BP) (Figure 1D and 1E), and human antigen R (HuR) (98.8% colocalized with RIG-I) (data not shown). Furthermore, physical interaction between RIG-I and SG markers was demonstrated by pull-down assays (Figure 1F). These results strongly suggest that although IAV infection potentially induces signaling to activate the IFN gene and the formation of granular aggregates containing SG markers, NS1 strongly blocks both. Ectopic expression of full-length NS1 and the N-terminal RNA-binding domain of NS1 dramatically inhibited both granule-formation and RIG-I signaling in response to IAVÄNS1 infection, indicating that the N-terminal domain of NS1 is responsible for these activities (Figure S2A and S2B).

SGs are an intracellular ribonucleoprotein (RNP) complex generated by cellular stress, including oxidative, heat shock, and endoplasmic reticulum stress, and contain translation-stalled mRNAs and various RNA-binding proteins [15]. Because many of the SG markers are RNA-binding proteins, we examined the localization of other RLRs, MDA5, and LGP2, as well as PKR (see below), RNase L, and OAS by using specific antibodies. Interestingly, these proteins were also recruited to SG and virus-induced granules in response to arsenite and IAVÄNS1, respectively (Figure 2A, 2B, 2C, 2D).

IAVÄNS1 Infection Induces Antiviral SGs Containing Viral RNA

These results prompted us to examine correlation between the formation of SGs and activation of the IFN gene. Treatment of cells with arsenite ($NaAsO_2$), which induced oxidative stress, produced granules similar to those generated by IAVÄNS1 (Figure 3A). Similarly, artificial overexpression of PKR resulted in the formation of SGs (58.9%) (Figure 3A). Although IAVÄNS1 infection activated the IFN-â gene, neither arsenite nor PKR activated the gene (Figure 3B). These results suggest that SGs and virus-induced granules are functionally distinct, possibly due to the presence of viral RNA in virus-induced granules. Indeed, fluorescence *in situ* hybridization (FISH) clearly demonstrated that viral RNA colocalized with the granules of NP (Figure 3C) and RIG-I (Figure 3D) in IAVÄNS1-infected cells whereas IAV-infected cells showed colocalization of viral RNA with NP (Figure S3A) but not with RIG-I (Figure S3B). Once viral RNA is engaged by RIG-I-containing complex, IFN-â promoter stimulator-1 (IPS-1, also known as MAVS, VISA or Cardif) expressed on the outer membrane of mitochondria is recruited to facilitate RIG-I-IPS1 signaling in a Mitofusin 1-dependent manner [12,16]. Although most of IPS-1 localizes on mitochondrial network in uninfected and IAV-infected cells, IAVÄNS1 infection induces speckle-like distribution. The re-localized IPS-1 exhibits apparent contacts with TIAR- (Figure 3E, bottom-right panel), and RIG-I- (Figure S4) containing SGs. This is consistent with a model that SG physically contacts with mitochondrion mediated by interaction between RIG-I and IPS-1 through caspase recruitment domain (CARD)-CARD homotypic interaction [17–20]. Although association of FLAG-tagged IPS-1 with peroxisome membrane protein (PMP70)-positive peroxisomes after viral infection was reported [21], we did not observe their apparent association (Figure 3E).

SG production is not a result of RIG-I signaling or IFN signaling because overexpression of IPS-1 activated the nuclear translocation of IRF-3 without generating SGs (Figure S5A), and SGs formed in IFN receptor-deficient HEC-1B cells (Figure S5B). Furthermore, other viruses including Sindbis (SINV), encephalomyocarditis (EMCV), and Adeno (Ad) dl203 viruses also generated granules containing RIG-I and G3BP (Figure S5C), suggesting this SG-like granule to be a general response to viral infections. To

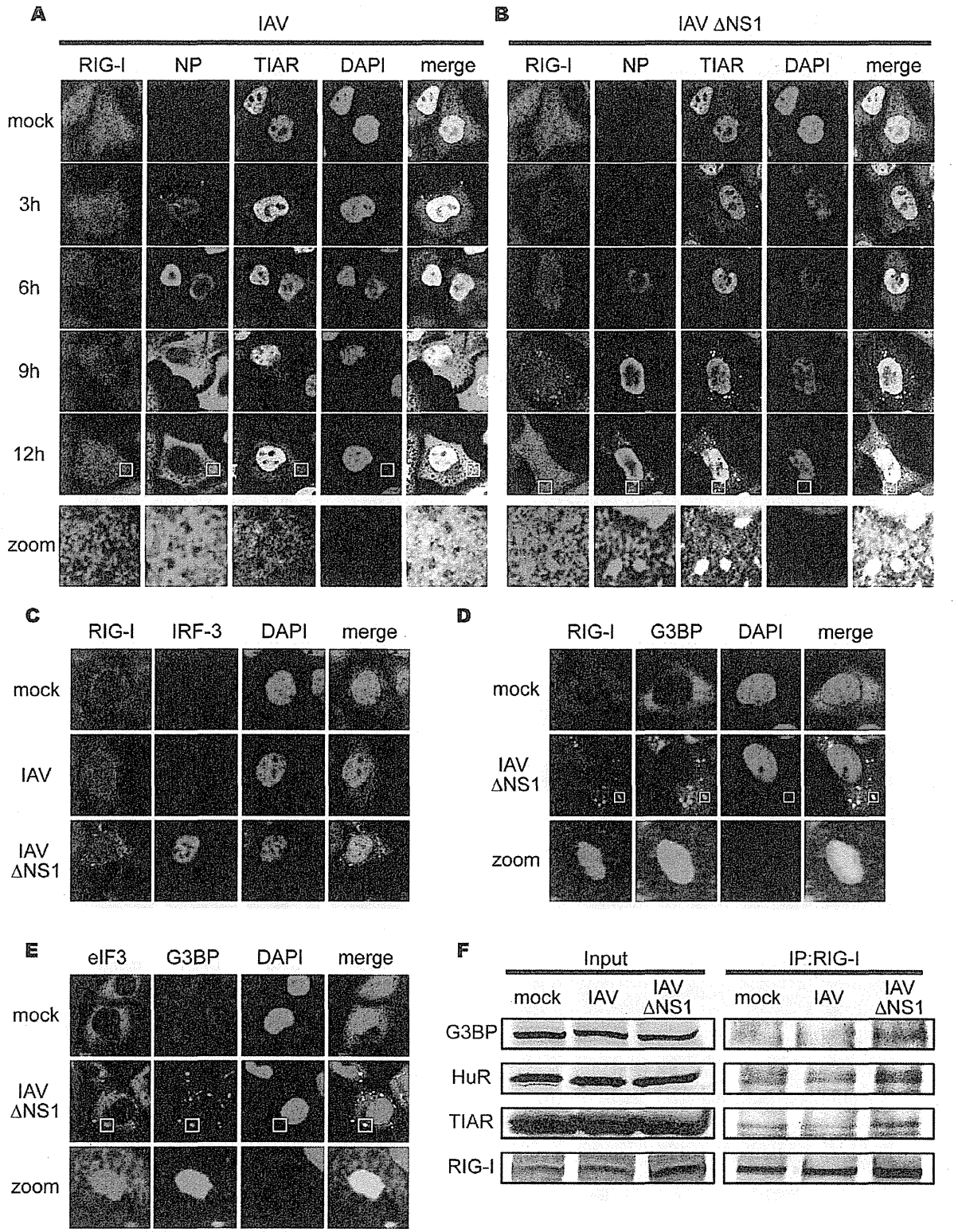

Figure 1. IAV infection causes a speckle-like distribution of RIG-I and stress granule markers. (**A–C**) HeLa cells were mock-treated or infected with IAV (**A**) or IAVΔNS1 (**B**) for the indicated period, fixed, stained, and analyzed with confocal microscopy. The cells were stained with anti-RIG-I (RIG-I), anti-IAV nucleocapsid protein (NP), and anti-TIAR (TIAR) antibodies. Nuclei were stained with DAPI. At 9 h and 12 h after infection, the

percentage of speckle-like distribution of RIG-I was 0.5% and 0.0% in IAV-infected cells, and 62.4% and 83.6% in IAVÄNS1-infected cells, respectively. The zoomed images correspond to the boxed region in each panel. The cells at 9 h post infection were stained with anti-RIG-I and anti-IRF-3 antibodies (**C**). (**D and E**) HeLa cells were infected with IAVÄNS1 for 9 h, and stained with anti-G3BP (G3BP), together with anti-RIG-I (RIG-I) (**D**) or anti-eIF3 (eIF3) (**E**). The zoomed images correspond to the boxed regions. (**F**) HeLa cells were mock-treated or infected with IAV or IAVÄNS1 for 12 h. Cell extracts were prepared and immunoprecipitated with anti-RIG-I antibody. The precipitates were analyzed by immunoblotting (IP:RIG-I) using antibody against G3BP, HuR, TIAR and RIG-I. Input: 1/50 of the extracts used for immunoprecipitation were analyzed similarly by immunoblotting.
doi:10.1371/journal.pone.0043031.g001

distinguish virus-induced granules from conventional SGs, we termed the virus-induced speckles as antiviral SGs (avSGs).

Impairment of Formation of avSGs Inhibits IAVÄNS1-induced IFN Activation

In order to address whether the formation of avSGs is required for IFN expression, we knocked down G3BP, a critical component for formation of the canonical SGs. G3BP siRNA clearly down-regulated G3BP expression (Figure 4A). Consistent with a previous study [22], the knockdown of G3BP strongly inhibited avSG formation in IAVÄNS1-infected cells (Figure 4B), and the number of cells which showed a speckle-like distribution of RIG-I and TIAR was diminished (Figure 4C and 4D). Moreover, IFN-â gene expression was strongly inhibited in G3BP knockdown cells compared to control siRNA-treated cells (Figure 4E). These results suggest that avSG formation is required for efficient activation of type I IFN. Furthermore, knockdown of eIF3 or RHAU, both of which are components of SG, also blocked both avSG formation and IFN gene activation (data not shown).

IAVÄNS1 Infection Induces PKR's Activation and Accumulation in avSGs

It has been proposed that a family of protein kinases including PKR, general control non-derepressible 2 (GCN2), PKR-like endoplasmic reticulum kinase (PERK), and heme-regulated eIF2á kinase (HRI) phosphorylate eIF2á, resulting in formation of SGs. Arsenite treatment causes oxidative stress leading to the activation of HRI, and SGs are produced. PKR is activated by dsRNA or 5¢ppp-containing RNA [23], therefore we speculate that the IAV RNA activates PKR resulting in the formation of avSGs via the phosphorylation of eIF2á. To address the involvement of PKR, we examined the localization of PKR in arsenite-treated and IAVÄNS1-infected cells and found that PKR accumulated in SGs and avSGs (Figure 5A). Interestingly, phosphorylated eIF2á was also detected in avSGs specifically generated by IAVÄNS1 but not in IAV-infected cells (Figure 5B). Immunoblotting confirmed that IAVÄNS1 specifically induced the phosphorylation of PKR and eIF2á whereas arsenite treatment induced the phosphorylation of eIF2á without PKR activation, indicating that IAVÄNS1 and arsenite induce SGs via distinct pathways (Figure 5C).

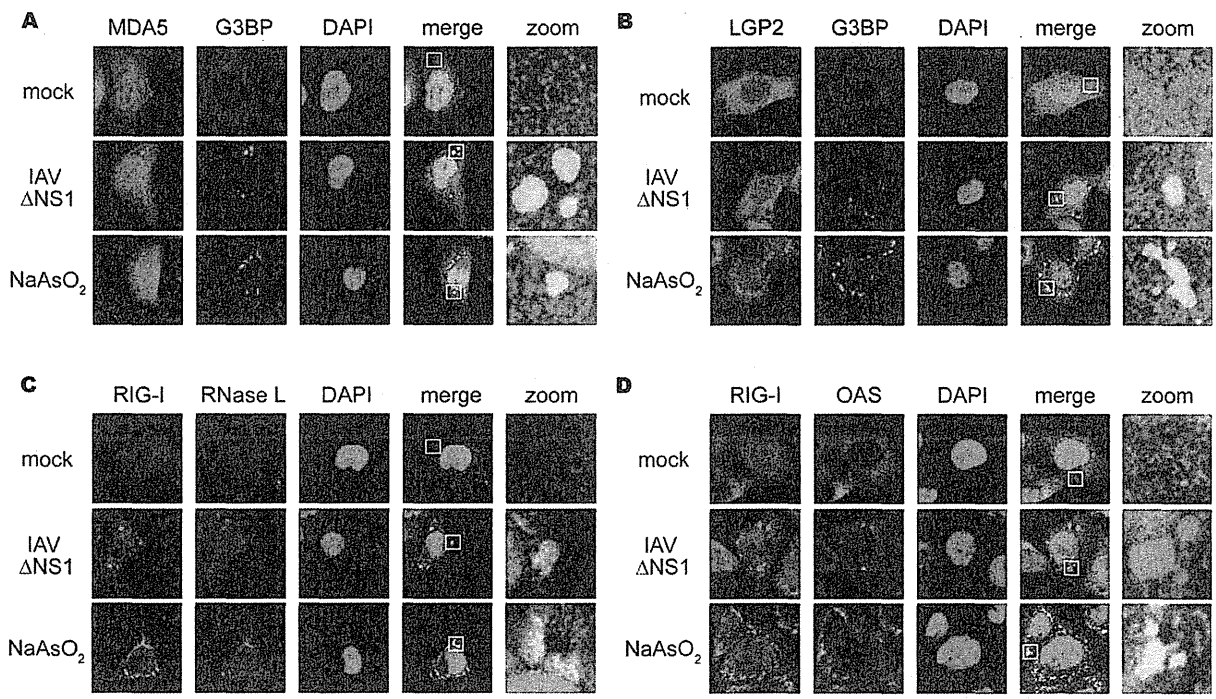

Figure 2. Antiviral proteins are colocalized with SGs. (**A–D**) HeLa cells were mock-treated (mock), infected with IAVÄNS1 for 9 h, or treated with $NaAsO_2$ for 1 h. Cells were fixed and stained for G3BP and MDA5 (94.2% colocalization) (**A**), G3BP and LGP2 (97.6% colocalization) (**B**), RIG-I and RNase L (84.5% colocalization) (**C**), RIG-I and OAS (87.4% colocalization) (**D**) in IAVÄNS1-infected cells. The zoomed images correspond to the boxed regions.
doi:10.1371/journal.pone.0043031.g002